NACA RM L53C20

NACA

RESEARCH MEMORANDUM

AERODYNAMIC CHARACTERISTICS AT HIGH AND LOW SUBSONIC MACH NUMBERS OF FOUR NACA 6-SERIES AIRFOIL SECTIONS AT ANGLES OF ATTACK FROM -2° TO 31°

By Homer B. Wilson, Jr., and Elmer A. Horton

Langley Aeronautical Laboratory
Langley Field, Va.

NATIONAL ADVISORY COMMITTEE
FOR AERONAUTICS

WASHINGTON

June 5, 1953

NACA RM L53C20

NATIONAL ADVISORY COMMITTEE FOR AERONAUTICS

RESEARCH MEMORANDUM

AERODYNAMIC CHARACTERISTICS AT HIGH AND LOW SUBSONIC MACH NUMBERS OF FOUR NACA 6-SERIES AIRFOIL SECTIONS AT ANGLES OF ATTACK FROM -2° TO 31°

By Homer B. Wilson, Jr., and Elmer A. Horton

SUMMARY

A two-dimensional wind-tunnel investigation has been made of four symmetrical NACA 6-series airfoil sections, 6, 8, 10, and 12 percent chord thick in the Langley low-turbulence pressure tunnel for Mach numbers from 0.3 to that for tunnel choke and for angles of attack from -2° to 31°. The results of the tests indicate that, for Mach numbers up to about 0.7, the section lift characteristics are essentially independent of airfoil thickness within the range of thickness ratios and angles of attack tested, except for the higher maximum lift coefficient exhibited by the NACA 64_1-012 airfoil section. The results also indicate that the section drag characteristics were comparatively independent of airfoil thickness within the range of Mach numbers tested for angles of attack above a value of about 8° greater than that for initial stall.

The position of the center of pressure was approximately constant at the 25-percent-chord station for angles of attack up to about 8° for the range of Mach numbers investigated. Increasing the angle of attack from about 8° to approximately 16° resulted in a rearward shift in the position of the center of pressure to about the 42-percent-chord station where it remained approximately constant to an angle of attack of 30° or 31°. The effect of Mach number is to produce a more gradual rearward shift in the position of the center of pressure. The break in the curve of pitching moment plotted against angle of attack was stable in all cases. It appears that the divergence Mach number is slightly higher for the pitching-moment coefficient than for the drag coefficient.

The addition of leading-edge roughness to the airfoil section resulted in a noticeable reduction in maximum lift at high subsonic Mach numbers and a large increase in the drag coefficient for angles of attack below stall. At angles of attack greater than that for initial stall, the addition of leading-edge roughness did not result in any significant changes in the aerodynamic characteristics throughout the range of Mach number investigated.

INTRODUCTION

The increasing speed of helicopters and consequently their rotor blades has intensified the need for airfoil section data at high subsonic Mach numbers throughout the angle-of-attack range at which the helicopter rotor blades operate. Although numerous high-speed airfoil section data are available through a limited angle-of-attack range, no high-speed data exist for angle-of-attack and Mach number combinations which may be encountered in certain high-speed-rotor design conditions. An investigation has therefore been made in the Langley low-turbulence pressure tunnel to provide airfoil section data through a wide range of angle of attack for a series of airfoil sections which might be used in helicopter rotor blades. The airfoil sections tested, which differ only in thickness ratio, were the NACA 64-006, 64-008, 64-010, and 64_1-012. Lift, drag, and pitching-moment data were obtained for Mach numbers of 0.3 to that for tunnel choke at angles of attack of -2° to 31°. The results of this investigation are reported herein.

SYMBOLS

c_l	section lift coefficient, l/qc
l	section lift, lb/ft of span
c	airfoil chord, ft
q	free-stream dynamic pressure, $\rho V^2/2$, lb/sq ft
V	free-stream velocity, ft/sec
ρ	free-stream mass density, slugs/cu ft
$c_{l_{max}}$	maximum section lift coefficient before stall
c_{d_o}	section drag coefficient, d/qc
d	section drag, lb/ft of span
$c_{m_{c/4}}$	section pitching-moment coefficient about quarter-chord point
α_o	section angle of attack, deg
R	Reynolds number based on airfoil chord and free-stream velocity

M	free-stream Mach number, V/a
a	free-stream speed of sound, ft/sec
P_s	stagnation pressure, in. Hg
T_s	stagnation temperature, $^{\circ}F$

APPARATUS, TESTS, AND METHODS

Wind tunnel.- The present investigation was conducted in the Langley low-turbulence pressure tunnel which has a test section 3 feet wide and $7\frac{1}{2}$ feet high. This tunnel was originally designed and has been operated for a number of years as a low-speed, high Reynolds number facility. At the present time, the tunnel is also operated as a high-speed research facility with Freon-12 gas replacing air as the test medium. Since the speed of sound in Freon is only about one-half of that in air, choking Mach numbers can be obtained in the test section with the original drive motor.

For the present investigation, the Mach number varied from approximately 0.3 to that for tunnel choke. The range of Reynolds numbers was determined by the absolute pressure of the tunnel. The present investigation was conducted at absolute pressures of approximately 6 and 11 inches of mercury and with a Freon purity of approximately 95 percent by weight. The variation of the Reynolds number per foot of chord with Mach number obtainable at the two tunnel pressures is shown in figure 1.

Models and test methods.- Each of the two-dimensional models tested in the investigation had a 1-foot chord and completely spanned the 3-foot dimension of the tunnel. The NACA 64-006 section was machined from solid steel and the NACA 64-008, NACA 64-010, and NACA 64_1-012 sections were machined from solid dural. The ordinates for each of the sections are presented in table I. A photograph of one of the models mounted in the tunnel is shown in figure 2. The ends of the model passed through slots in the tunnel walls; one end of the model was mounted through a universal joint to a semispan balance and the other end was pivoted in a self-alining bearing. A labyrinth-type seal was provided at each end of the model to minimize the effect of leakage through the slots in the tunnel walls. With this mounting arrangement, the model is essentially a simply supported beam in both the lift and drag directions and free of restraint in roll and yaw (as far as the balance is concerned). Thus, the semispan balance measures one-half the lift and drag and all of the pitching moment. A sketch showing the relationship between the ends

of the model, the tunnel wall, the labyrinth seal, the mounting pivot, and balance is presented in figure 3.

The semispan balance was employed for making all the lift, drag, and pitching-moment measurements of the present investigation. The lift and drag as measured by the semispan balance have been shown in reference 1 to be in good agreement with the lift and drag determined by integrating the pressures along the floor and ceiling of the tunnel and the wake-survey method, respectively.

Tests.- The investigation consisted of measurements of the lift, drag, and pitching-moment of the NACA 64-006, 64-008, 64-010, and 64_1-012 airfoil sections through an angle-of-attack range of -2° to 31°. The Mach number varied from 0.3 to that for tunnel choke. The Mach number for tunnel choke is shown in figure 4 as a function of angle of attack and model thickness ratio. Because of the limitations of the semispan balance, the tests were made at two stagnation pressures, that is, for two ranges of Reynolds number. The Reynolds number is shown in figure 1 as a function of Mach number for a constant stagnation temperature and the two stagnation pressures used in this investigation. For angles of attack of -2° to 13°, a stagnation pressure of about 11 inches of mercury was used and the Reynolds number varied from approximately 2.0×10^6 to 5.0×10^6. For angles of attack of 13° to 31°, a stagnation pressure of about 6 inches of mercury was used and the Reynolds number varied from approximately 1.0×10^6 to 2.3×10^6. The correspondence between Reynolds number and Mach number shown in figure 4 does not necessarily represent the exact test conditions of the present investigation because of variations in stagnation temperature, total pressure, and Freon purity.

Measurements were made of the lift, drag, and pitching moments for the models in the aerodynamically smooth condition and with leading-edge roughness. The leading-edge roughness consisted of 0.011-inch-diameter carborundum grains spread over a surface length of 8 percent of the chord back from the leading edge on the upper and lower surfaces. The grains were thinly spread to cover from 5 to 10 percent of this area. One model, the NACA 64_1-012 airfoil section, was also tested with a strip of roughness extending chordwise for 1/4 inch along the upper and lower surfaces of the model beginning at the 20-percent-chord station.

Corrections.- All the data presented herein have been corrected for tunnel wall effects according to the methods of references 2 and 3. The maximum tunnel wall corrections were of the order of 9 percent for the lift, drag, and pitching-moment coefficient. Corrections were also applied to all data of the present investigation to convert the data obtained in Freon to equivalent air data. These corrections are discussed in reference 4. The magnitude of the corrections was rather small. For example, the measured Freon Mach number differed by only about 3.0 percent

from its equivalent air Mach number and the measured lift, drag, and pitching-moment coefficient differed by as little as 5, 3, and 4 percent, respectively, from their equivalent values in air. The highest Mach numbers for which data are presented correspond to the tunnel choked condition. The highest Mach number for which the data may be considered reliable is open to some question. A Mach number of 0.03 less than that for choke, however, has oftentimes been considered as a rough upper limit beyond which little confidence should be placed in the results.

Precision of measurement.- The balance employed in the present investigation was designed to measure drag forces to within 1/2 pound, lift forces to within 1.5 pound, and pitching moments to within 3 inch-pounds. On the basis of these limits, the accuracy of the measurements for various test conditions is indicated in the following table:

Accuracy of Measurements				
M (approx.)	q, lb/sq ft	c_l	c_{d_o}	$c_{m_{c/4}}$
0.3	35	±0.013	±0.0030	±0.003
.67	175	±.003	±.0006	±.001
.85	260	±.002	±.0004	±.001

For steady flow conditions, that is, for angles of attack below the stall, the repeatability of the data and the comparison of results for the different airfoils indicated that the accuracy of the measurements was considerably better than is indicated by the preceding table.

In the early stages of the investigation, it was noted that the variation of the force and moment coefficients with Mach number was somewhat erratic for angles of attack in the vicinity of and above the stall. In an attempt to obtain an average variation of the force and moment coefficients with Mach number, the force and moment coefficients were measured at 0.005 increments in Mach number. The curves presented herein represent an average of the data obtained with some typical data points plotted. The scatter of the most random data points (not shown) was approximately ±5 percent of the faired curves of the lift, drag, and pitching-moment coefficients. Most of the data points, however, fell within a band about ±2 percent of the faired curves.

RESULTS

The test results are presented in figures 5 to 8 in the form of standard coefficients representing the lift, drag, and pitching moment (about the quarter chord) plotted against Mach number at Reynolds numbers varying from 1.0×10^6 to 5.0×10^6 and Mach numbers varying from approximately 0.3 to that for tunnel choke. To facilitate the use of the data, the following additional figures (9 to 16) have been prepared using Mach number as the parameter: section lift coefficient (fig. 9), section drag coefficient (fig. 11), and the chordwise position of the center of pressure (figs. 9 and 14) plotted against angle of attack; section pitching-moment coefficients (about the quarter chord) (figs. 12 and 13), and section drag coefficient (figs. 15 and 16) plotted against lift coefficient. The lift-curve slope as a function of Mach number is presented in figure 10.

DISCUSSION

Lift Coefficient

The variation of the section lift with Mach number for all airfoil sections tested is shown by figures 5(a), 6(a), 7(a), and 8(a). For angles of attack up to about 14°, the lift coefficient is relatively independent of Mach number up to values as high as 0.65 to 0.75. For these angles further increase in the Mach number resulted in a sharp increase in the lift coefficient up to the divergence Mach number after which the lift coefficient decreased with increasing Mach number and continued to decrease with increasing Mach number up to the highest Mach number attained in this investigation. At angles of attack of 14° to 22°, the variation of the lift coefficient with Mach number is somewhat erratic, but indicates a general increase with Mach number. For angles of attack above 22° the curves are less erratic but show the same general increase in lift coefficient with Mach number. At an angle of attack of 13° or 14°, data were taken for the two ranges of Reynolds number. The results did not show any consistent variation of the coefficients with Reynolds number.

Lift-curve slope.- The increase in lift-curve slope, usually associated with an increase in Mach number is shown in figure 10, which is a plot of $\left(\frac{dc_l}{d\alpha_o}\right)_{\alpha=0^\circ}$ as a function of Mach number for the airfoil sections tested. The slope of the lift curve (fig. 9) is essentially constant from 0° to 8° and increases with increasing Mach number for all airfoil

sections tested. For example, increasing the Mach number from 0.3 to 0.8 increased the value of $\left(\frac{dc_l}{d\alpha_o}\right)_{\alpha=0^\circ}$ from 0.11 per degree to 0.21 per degree for the NACA 64-006 airfoil section (fig. 10). The incremental increase in the value of $\left(\frac{dc_l}{d\alpha_o}\right)_{\alpha=0^\circ}$ seems to be relatively independent of the thickness of the airfoil section for Mach numbers less than 0.75.

For angles of attack above about 8°, the slope of the lift curves decreased with increasing angles of attack to stall (fig. 9). As would be expected, the value of $dc_l/d\alpha_o$ becomes negative after stall or maximum lift, and remains negative for angles of attack approximately 8° above that for stall. A further increase in the angle of attack results in a positive but varying value of $dc_l/d\alpha_o$ which remains positive to the highest angle of attack attained in this investigation.

Maximum lift coefficient.- The increase in the maximum lift coefficient (the highest lift coefficient obtained before stall) as the thickness ratio is increased from 6 to 12 percent chord for Mach numbers less than 0.15 reported in the investigation of reference 2 was not shown in this investigation for a Mach number of 0.3 (fig. 9). This decrease in the effect of increasing thickness on maximum lift coefficient is shown in reference 5 to be a result of increasing Mach number. For example, figure 6 of reference 5 shows that increasing the Mach number from 0.10 to 0.30 resulted in a decrease in the maximum lift coefficient of moderately thick airfoil sections and a substantial reduction in the effect of thickness on the maximum lift coefficient at Reynolds number approximately equal to those of the present investigation. In view of these results from reference 5, the absence of substantial increase in the maximum lift coefficient with increasing thickness at $M = 0.3$, shown by the data of figure 9, was to be expected. For a constant thickness ratio, the maximum lift coefficient was also relatively unaffected for Mach numbers up to about 0.60; however, at Mach numbers greater than 0.60, the maximum lift coefficient showed a definite increase with increasing Mach number. The angle of attack for maximum lift generally decreased with increasing Mach number. For angles of attack greater than about 8° above the stall angle, the lift coefficient increased with increasing angle of attack and continued to increase to the maximum angle of attack obtained in this investigation. The value of the lift coefficient at the maximum angle of attack obtained in this investigation was in all cases greater than $c_{l_{max}}$.

The effect of increasing thickness on the lift characteristics of the airfoil sections tested is summarized in figure 11 for several Mach

numbers. These data indicate no consistent variation of the lift characteristics with increasing thickness for angles of attack greater than about 8° above that for stall; however, at stall, the NACA 64_1-012 airfoil section showed a slightly higher maximum lift coefficient for Mach numbers up to 0.6.

Pitching Moment

The variation with Mach number of the quarter-chord pitching-moment coefficient $c_{m_{c/4}}$ is shown in figures 5(c), 6(c), 7(c), and 8(c). The erratic variations shown in the lift curves for angles of attack between 16° and 22° are not as apparent in the pitching-moment curves. For angles of attack between 22° and 31°, no definite break in the pitching-moment curves occurred before the choke Mach number was reached. From a comparison of the data presented in figures 5 to 8, it appears that the divergence Mach number occurs at a slightly higher value for the pitching-moment coefficient than for the drag coefficient.

The variation of the pitching-moment coefficients about the quarter chord $c_{m_{c/4}}$ with lift coefficient is shown in figure 12. The values of the pitching-moment coefficient and the slope of the pitching-moment polar $\frac{dc_{m_{c/4}}}{dc_l}$ are constant and essentially zero for lift coefficients up to about 8 percent less than those for $c_{l_{max}}$ for Mach numbers less than 0.80. At a Mach number of 0.80, the value of $\frac{dc_{m_{c/4}}}{dc_l}$ is generally negative for all airfoil sections at lift coefficients up to about 8 percent less than that for stall. Increasing the lift coefficient to values in the vicinity of stall results in a break in the pitching-moment polar which in all cases was stable. At lift coefficients immediately above stall, the variation of the pitching moment is somewhat erratic; however, if the angle of attack is increased to values of about 8° or more above that for stall, the values of $\frac{dc_{m_{c/4}}}{dc_l}$ and $c_{m_{c/4}}$ are negative and varying but less erratic.

A comparison of the pitching-moment characteristics of all airfoil sections tested in the smooth condition is shown in figure 13. In general, these data indicate that the pitching-moment characteristics are essentially the same for all airfoil sections tested with the exception of a delayed break in the pitching-moment curve for the NACA 64_1-012 airfoil section for Mach numbers from 0.3 to 0.70.

Center of pressure.- The variation of the center-of-pressure position for all airfoil sections tested is shown in figure 9. Figure 14, a plot of the position of the center of pressure as a function of angle of attack for all the airfoils in the smooth condition, indicates that the position of the center of pressure is relatively constant at the 25-percent-chord station at angles of attack up to about 6° to 8° for all Mach numbers tested. For angles of attack from 6° to 8° to approximately 16°, the center of pressure shifts rearward, with the rearward shift being less for the thicker sections at low Mach numbers. At angles of attack above 16° the center of pressure is approximately constant at its most rearward position at about the 42-percent-chord station. Increasing the free-stream Mach number from 0.30 to 0.70 seems to result in a more gradual rearward shift in the position of the center of pressure. The effect of increasing thickness seems to be a slightly delayed break in the center-of-pressure curve for the NACA 64_1-012 airfoil section at Mach numbers less than 0.60. Otherwise there seems to be no significant difference in the center-of-pressure characteristics associated with increasing thickness ratio for the airfoil sections tested.

Drag Characteristics

The effect of increasing Mach number on the drag characteristics is shown in figures 5(b), 6(b), 7(b), and 8(b). At angles of attack of -2° to 15°, the drag coefficient is essentially independent of Mach number until the force-break Mach number is attained, then the drag coefficient increases rapidly. For angles of attack from 16° to 24°, the curves are somewhat erratic in variation but show a general increase of drag with Mach number. The same general increase in drag with Mach number is shown for angles of attack between 24° and 31° but the curves are less erratic than those for angles of attack of 16° to 24°.

The lift-drag polars for the four airfoil sections tested are presented in figure 15 for a series of Mach numbers. The polars are plotted with two different scales for each Mach number presented: One scale, the larger of the two, permits the comparison of the minimum drag characteristics of the models tested; whereas, the small scale was used in order to present the drag data for the complete range of lift coefficients investigated. The lift-drag polars, presented in figure 15 indicate a small increase in the minimum drag coefficient c_{d_o} with increasing thickness ratio and Mach number up to the divergence Mach number.

In order to aid in comparing the section drag characteristics through a complete range of angles of attack and lift coefficient, the

variations of section drag coefficient with angle of attack and lift coefficient for several Mach numbers are presented in figures 11 and 16, respectively. The data have been plotted to a small scale in order to show the high section drag coefficients at high lift coefficients and angles of attack since a comparison of the minimum drags can be obtained from figure 15. Figure 11, a plot of section drag coefficient of each of the airfoils investigated against angle of attack for several Mach numbers, shows that the shape of the section drag curves is essentially the same for all of the airfoil sections through the range of angle of attack and Mach numbers tested. The drag polars, shown in figure 16, indicate that the NACA 64_1-012 airfoil section has the largest lift-drag ratio for Mach numbers up to about 0.70 whereas for higher Mach numbers the NACA 64-006 airfoil section has, in general, the highest lift-drag ratio.

Effect of Roughness

Lift and pitching-moment characteristics.- The addition of roughness to the leading edge of the airfoil sections tested did not produce any significant effects on the lift characteristics at low subsonic Mach numbers (M = 0.3 to 0.5) for any of the four airfoil sections tested (fig. 9). Similar results were obtained in reference 5 in which the maximum lift coefficient of several roughened airfoils for Mach numbers as high as 0.45 was shown to be essentially unaffected by increasing Mach number. At high subsonic Mach numbers (M = 0.6 to 0.8), the addition of leading-edge roughness resulted in a noticeable reduction in the maximum lift coefficient (fig. 9) and consequently an earlier break in the pitching-moment curve (fig. 12) for all models tested. The addition of a spanwise roughness strip at the 20-percent-chord position on the NACA 64_1-012 airfoil section did not appreciably affect the lift, pitching-moment, or center-of-pressure characteristics throughout the Mach number range investigated.

Drag characteristics.- From figures 5(b), 6(b), 7(b), and 8(b), it is seen that the addition of leading-edge roughness had practically no effect on the drag divergence Mach number but did result in large increases in drag coefficient at Mach numbers below drag divergence, at least for the lower angles of attack below that for stall. For lift coefficients beyond that for stall, there is, in general, no consistent increase or decrease in the drag coefficient attributable to the addition of leading-edge roughness (fig. 15). The addition of a roughness strip at the 20-percent-chord station produces the same general effect on the drag characteristics as did leading-edge roughness, but is less severe.

CONCLUDING REMARKS

The NACA 64-006, 64-008, 64-010, and 64_1-012 airfoil sections have been investigated in the Langley low-turbulence pressure tunnel for Mach numbers from 0.3 to that for tunnel choke and for angles of attack from -2° to 31°. The results of the tests indicate that, for Mach numbers up to about 0.7, the section lift characteristics are essentially independent of airfoil thickness within the range of thickness ratios and angles of attack tested, except for the higher maximum lift coefficient exhibited by the NACA 64_1-012 airfoil section. The results also indicate that the section drag characteristics were comparatively independent of airfoil thickness within the range of Mach numbers tested for angles of attack above a value of about 8° greater than that for initial stall.

The position of the center of pressure was approximately constant at the 25-percent-chord station for angles of attack up to about 8° for the range of Mach numbers investigated. Increasing the angle of attack from about 8° to approximately 16° resulted in a rearward shift in the position of the center of pressure to about the 42-percent-chord station where it remained approximately constant to an angle of attack of 30° or 31°. The effect of Mach number is to produce a more gradual rearward shift in the position of the center of pressure. The break in curve of pitching moment plotted against angle of attack was stable in all cases. It appears that the divergence Mach number is slightly higher for the pitching-moment coefficient than for the drag coefficient.

The addition of leading-edge roughness to the airfoil section resulted in a noticeable reduction in maximum lift at high subsonic Mach numbers and a large increase in the drag coefficient for angles of attack below stall. At angles of attack greater than that for initial stall, the addition of leading-edge roughness did not result in any significant changes in the aerodynamic characteristics throughout the range of Mach numbers investigated.

Langley Aeronautical Laboratory,
National Advisory Committee for Aeronautics,
Langley Field, Va.

REFERENCES

1. Loftin, Laurence K., Jr., and Von Doenhoff, Albert E.: Exploratory Investigation at High and Low Subsonic Mach Numbers of Two Experimental 6-Percent-Thick Airfoil Sections Designed To Have High Maximum Lift Coefficients. NACA RM L51F06, 1951.

2. Abbott, Ira H., Von Doenhoff, Albert E., and Stivers, Louis S., Jr.: Summary of Airfoil Data. NACA Rep. 824, 1945. (Supersedes NACA WR L-560.)

3. Allen, H. Julian, and Vincenti, Walter G.: Wall Interference in a Two-Dimensional-Flow Wind Tunnel, With Consideration of the Effect of Compressibility. NACA Rep. 782, 1944. (Supersedes NACA WR A-63.)

4. Von Doenhoff, Albert E., and Braslow, Albert L.: Studies of the Use of Freon-12 As a Testing Medium in the Langley Low-Turbulence Pressure Tunnel. NACA RM L51I11, 1951.

5. Racisz, Stanley F.: Effects of Independent Variations of Mach Number and Reynolds Number on the Maximum Lift Coefficients of Four NACA 6-Series Airfoil Sections. NACA TN 2824, 1952.

TABLE I

COORDINATES OF NACA AIRFOIL SECTIONS TESTED

(Dimensions given in percent chord)

Chordwise station	Upper and lower surface ordinate			
	64-006	64-008	64-010	64_1-012
0	0	0	0	0
.5	.494	.658	.820	.978
.75	.596	.794	.989	1.179
1.25	.754	1.005	1.250	1.490
2.5	1.024	1.365	1.701	2.035
5	1.405	1.875	2.343	2.810
7.5	1.692	2.259	2.826	3.394
10	1.928	2.574	3.221	3.871
15	2.298	3.069	3.842	4.620
20	2.572	3.437	4.302	5.173
25	2.772	3.704	4.639	5.576
30	2.907	3.884	4.864	5.844
35	2.981	3.979	4.980	5.978
40	2.995	3.992	4.988	5.981
45	2.919	3.883	4.843	5.798
50	2.775	3.684	4.586	5.480
55	2.575	3.411	4.238	5.056
60	2.331	3.081	3.820	4.548
65	2.050	2.704	3.345	3.974
70	1.740	2.291	2.827	3.350
75	1.412	1.854	2.281	2.695
80	1.072	1.404	1.722	2.029
85	.737	.961	1.176	1.382
90	.423	.550	.671	.786
95	.157	.206	.248	.288
100	0	0	0	0
L. E. rad.	0.256	0.455	0.720	1.040

NACA

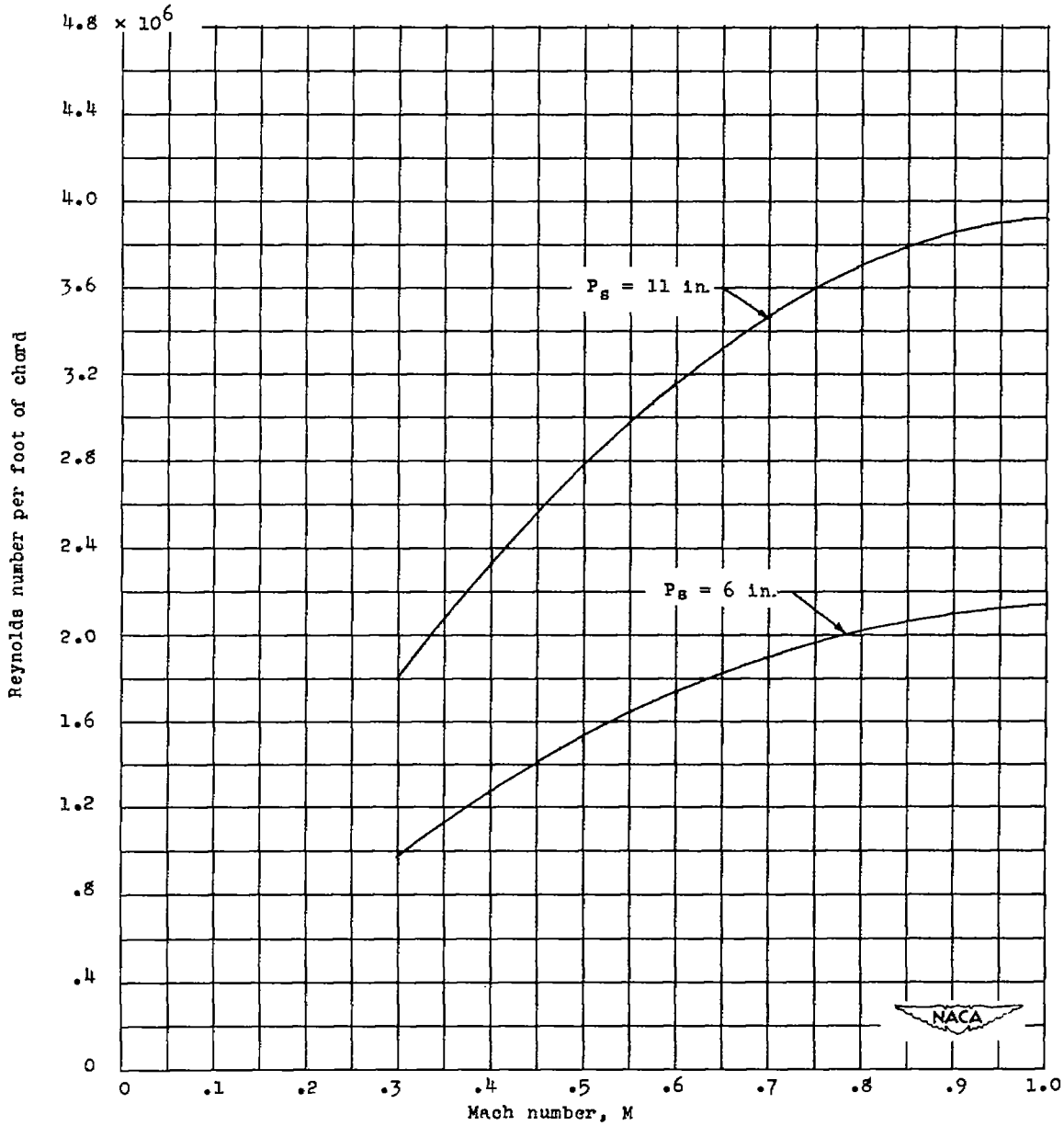

Figure 1.- Variation of Reynolds number per foot of chord with Mach number for various stagnation pressures P_s in inches of mercury and a stagnation temperature T_s of 70° F.

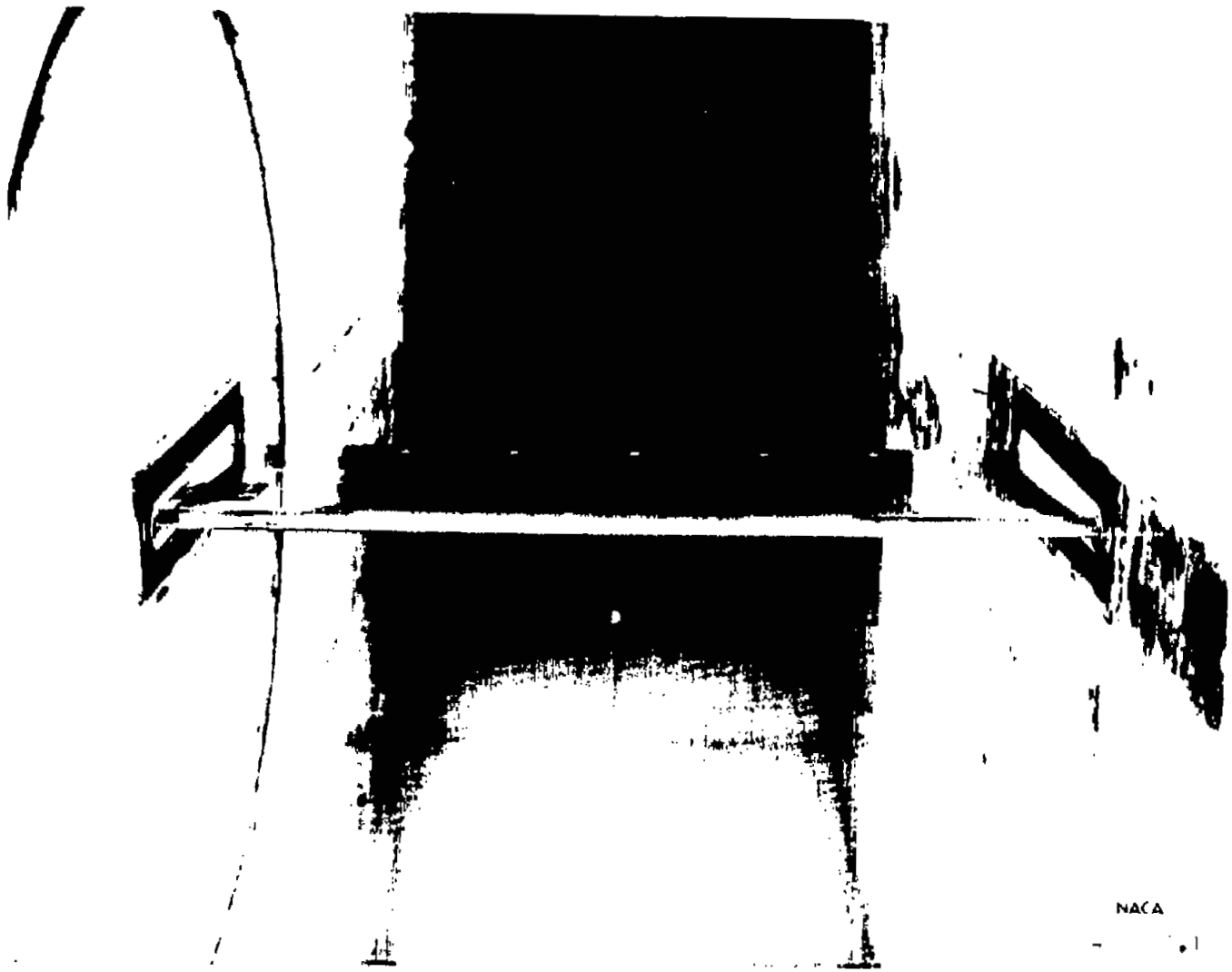

Figure 2.- Photograph of a model as mounted in the Langley low-turbulence pressure tunnel.

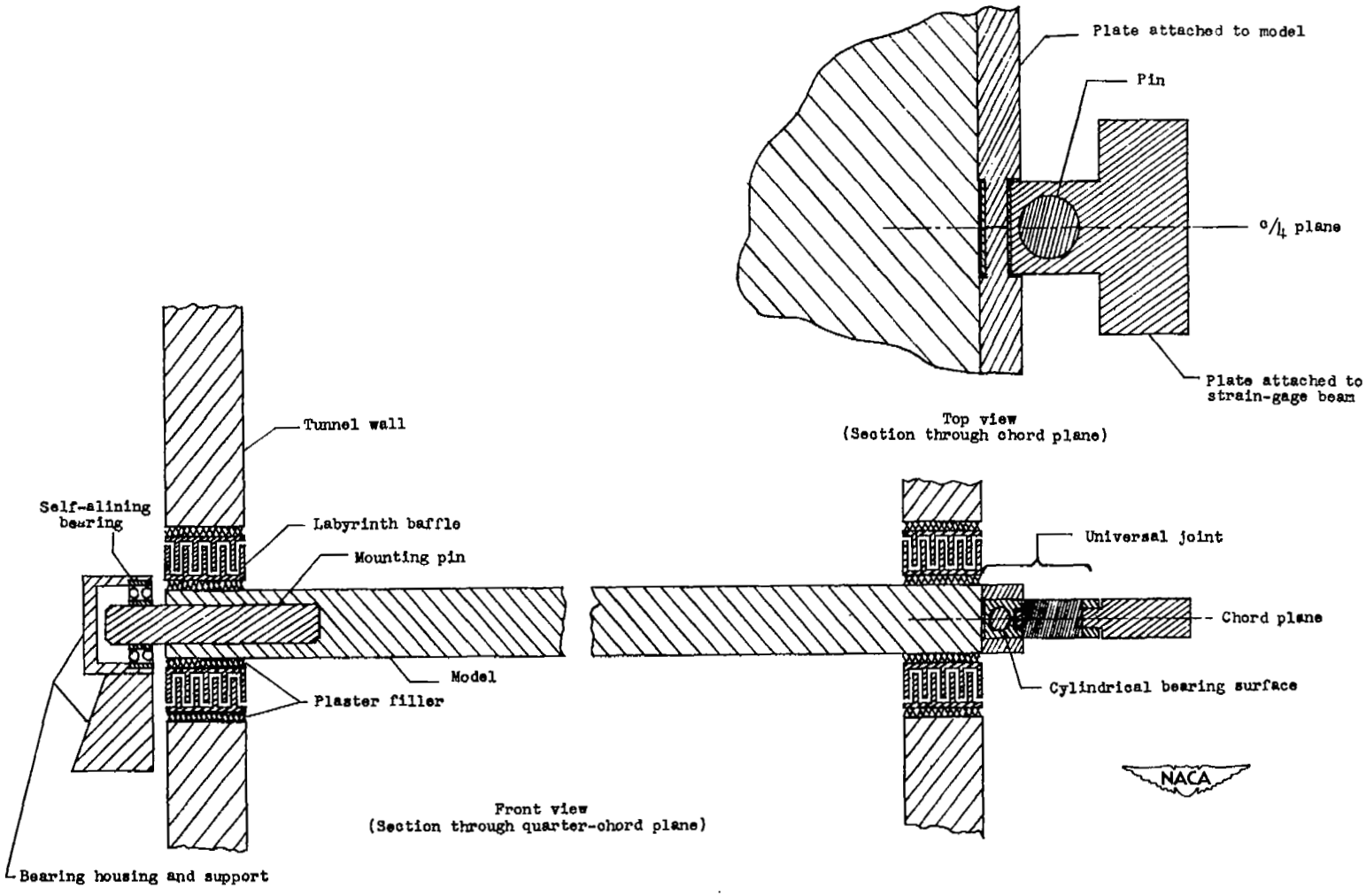

Figure 3.- Schematic drawing of model mounted in tunnel for force and moment measurements employing strain-gage balance.

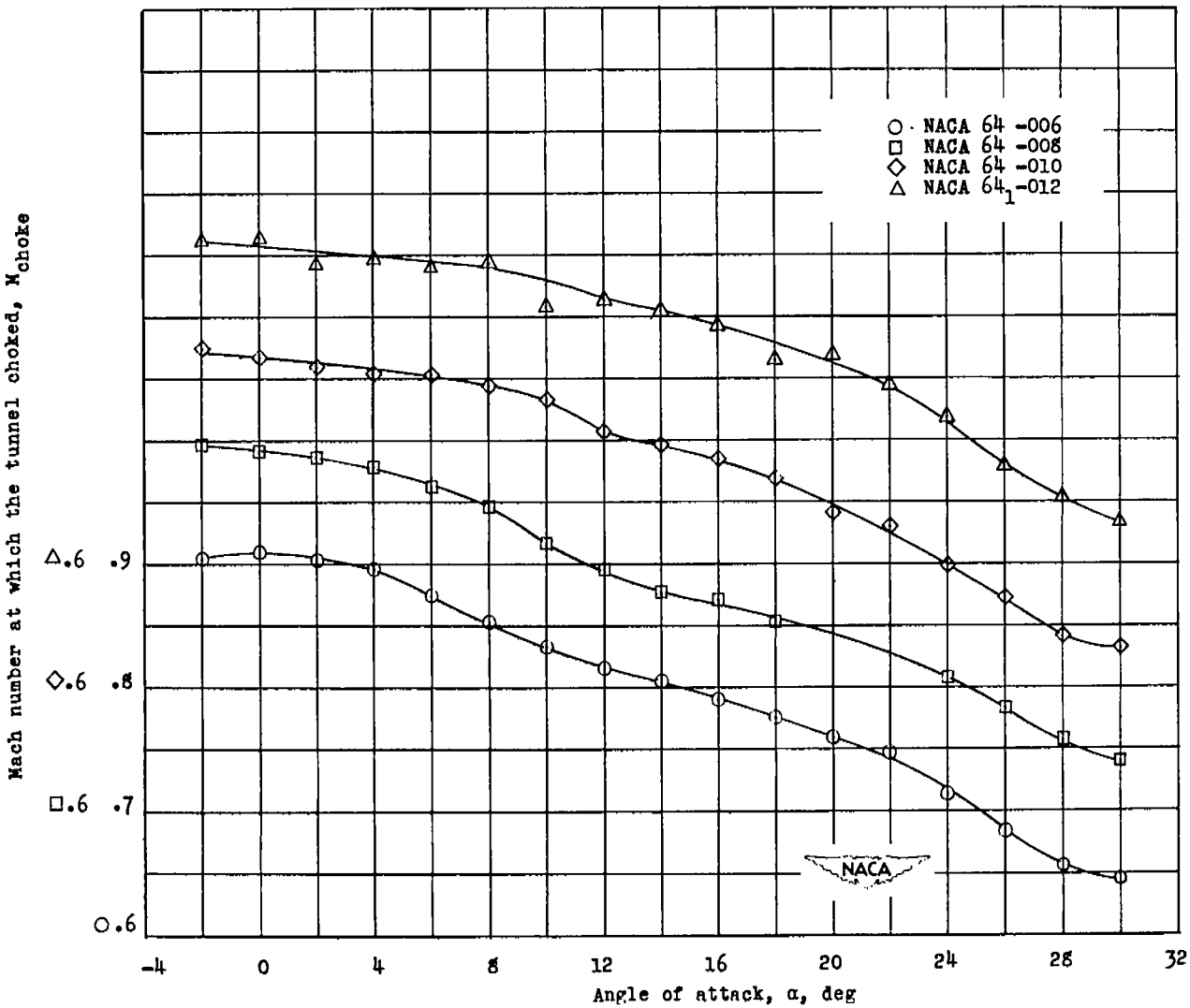

Figure 4.- Variation of the Mach number at which the tunnel choked with angle of attack for four NACA 6-series airfoil sections.

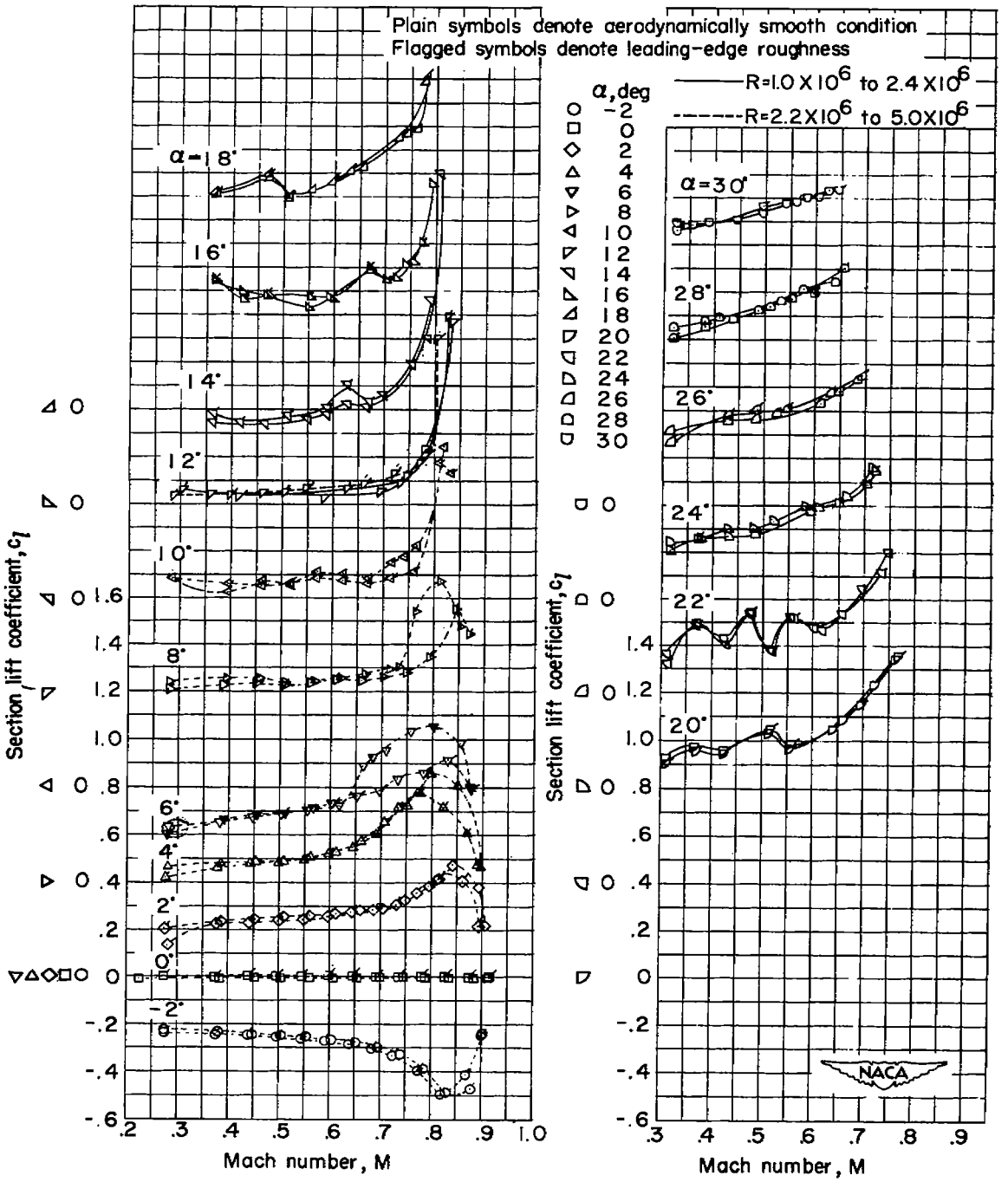

(a) Variation of section lift coefficient with free-stream Mach number.

Figure 5.- Effect of leading-edge roughness upon the high-speed aerodynamic characteristics of the NACA 64-006 airfoil section at various angles of attack.

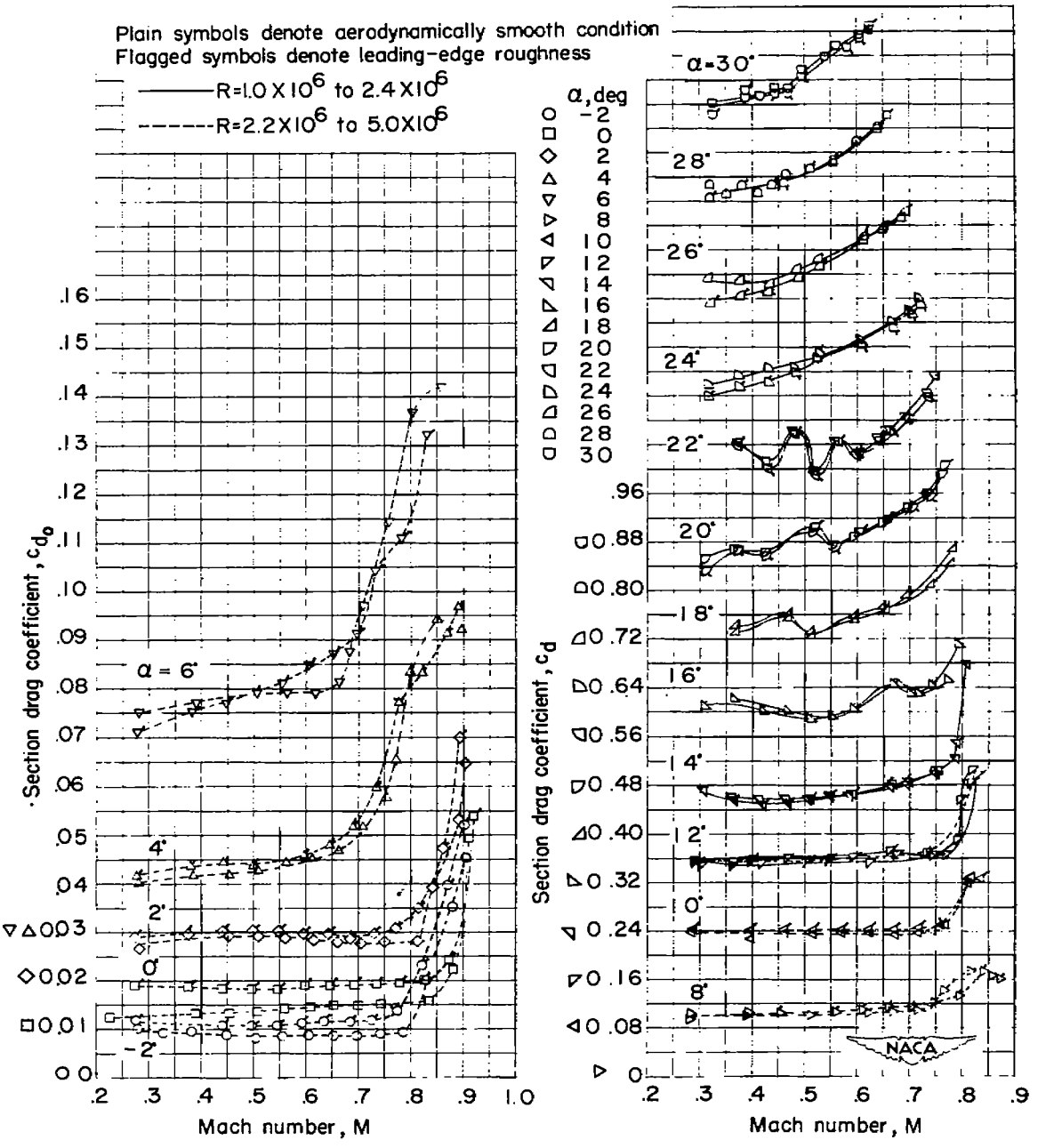

(b) Variation of section drag coefficient with free-stream Mach number.

Figure 5.- Continued.

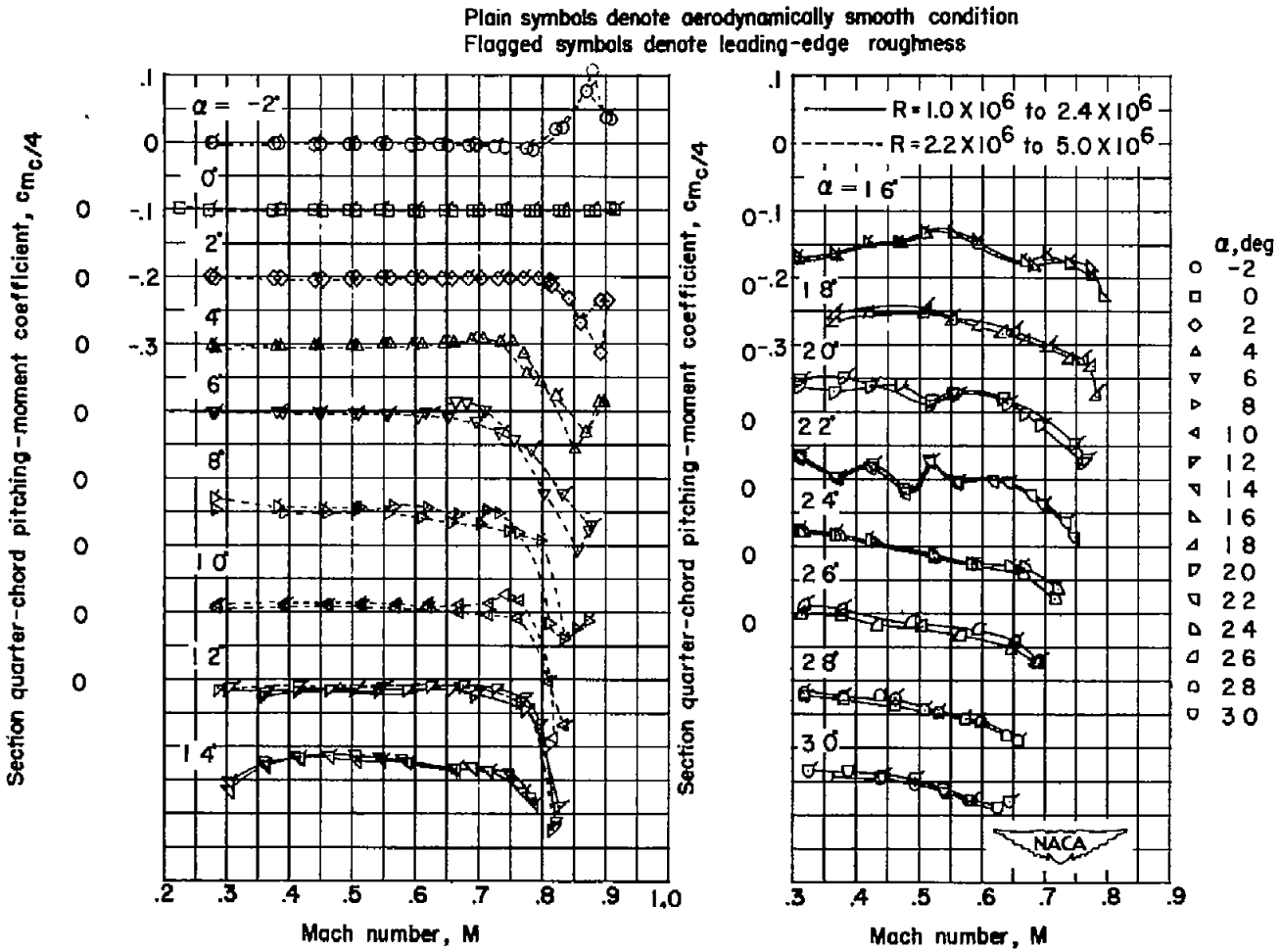

(c) Variation of section quarter-chord pitching-moment coefficient with free-stream Mach number.

Figure 5.- Concluded.

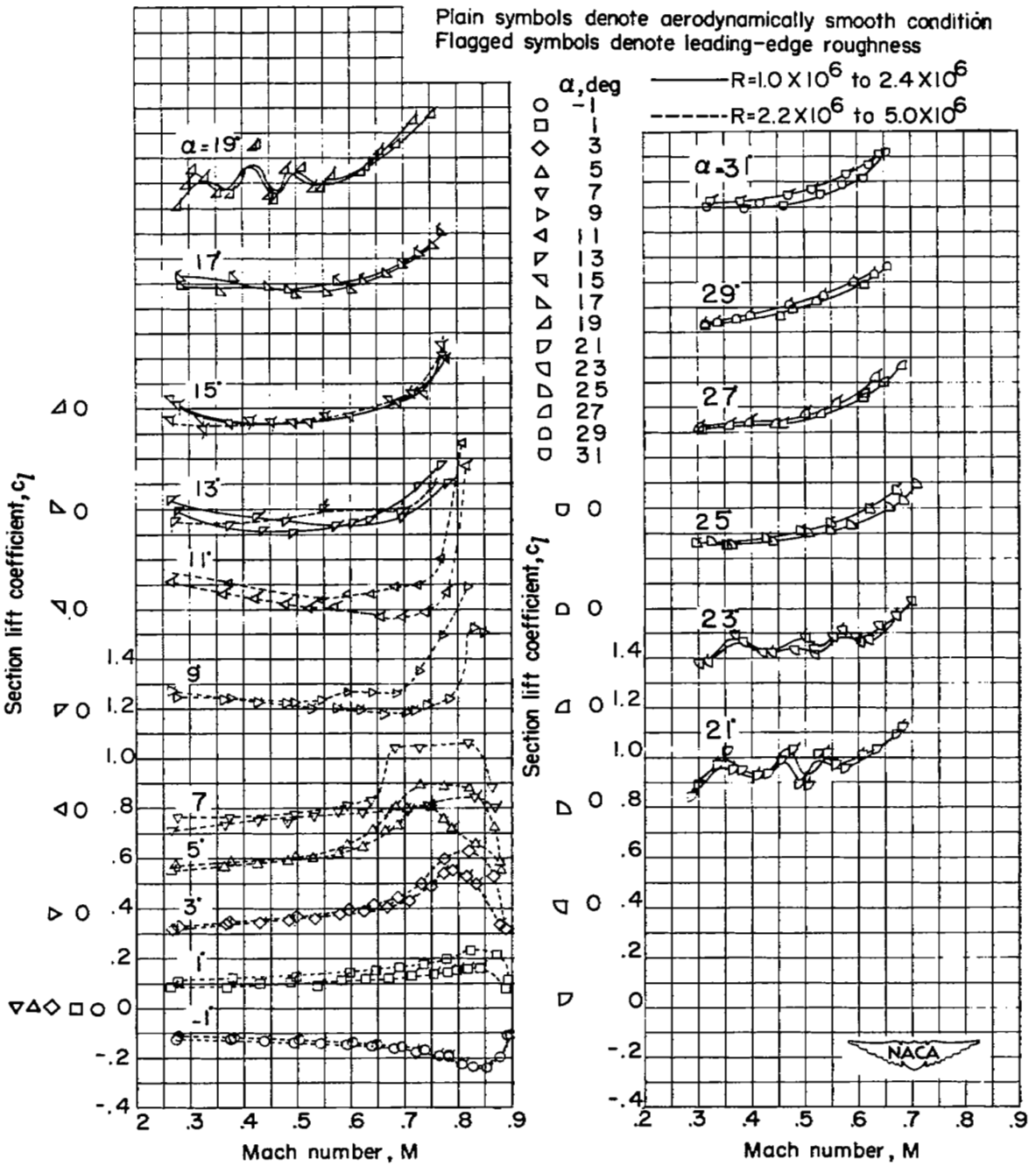

(a) Variation of section lift coefficient with free-stream Mach number.

Figure 6.- Effect of leading-edge roughness upon the high-speed aerodynamic characteristics of the NACA 64-008 airfoil section at various angles of attack.

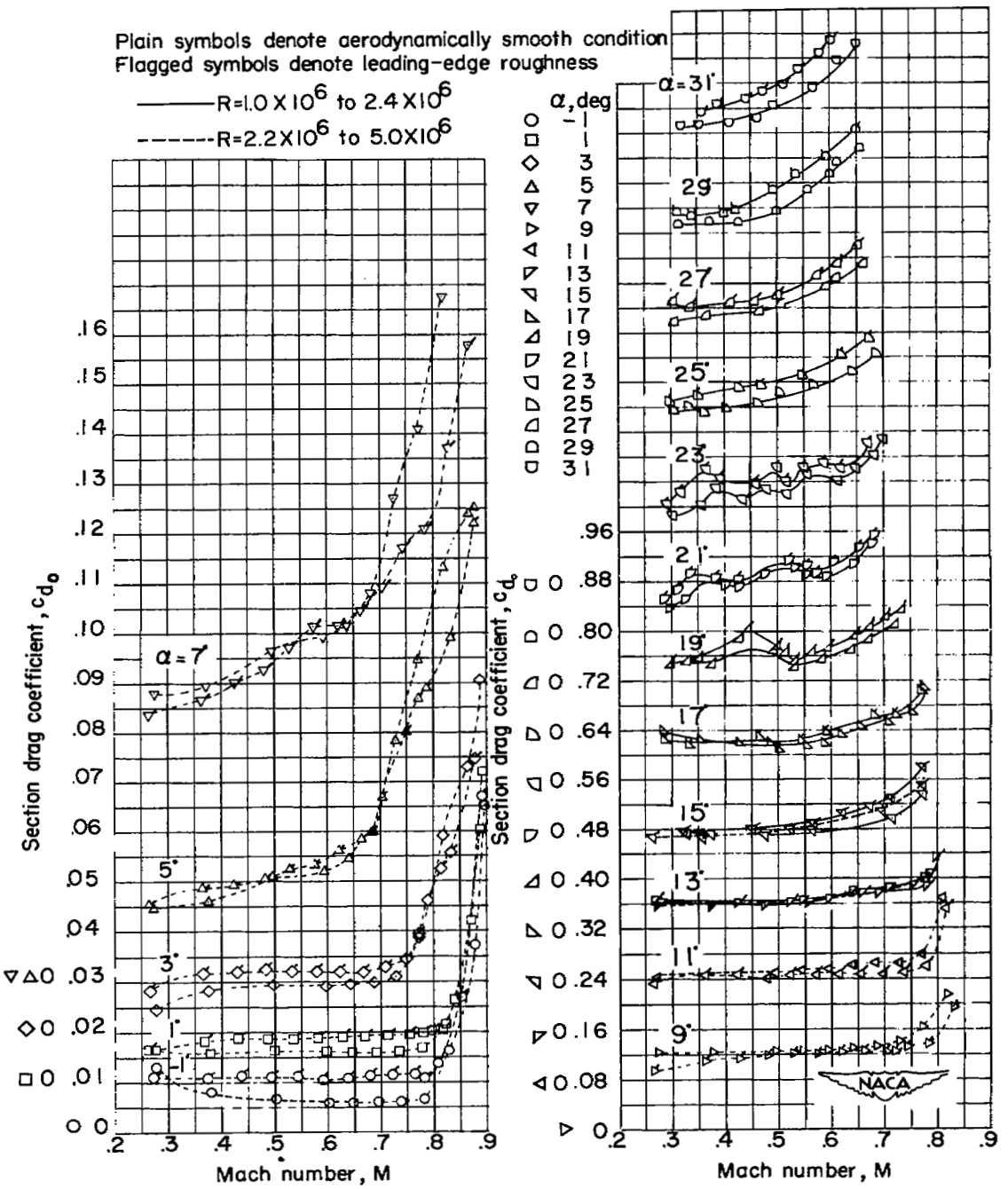

(b) Variation of section drag coefficient with free-stream Mach number.

Figure 6.- Continued.

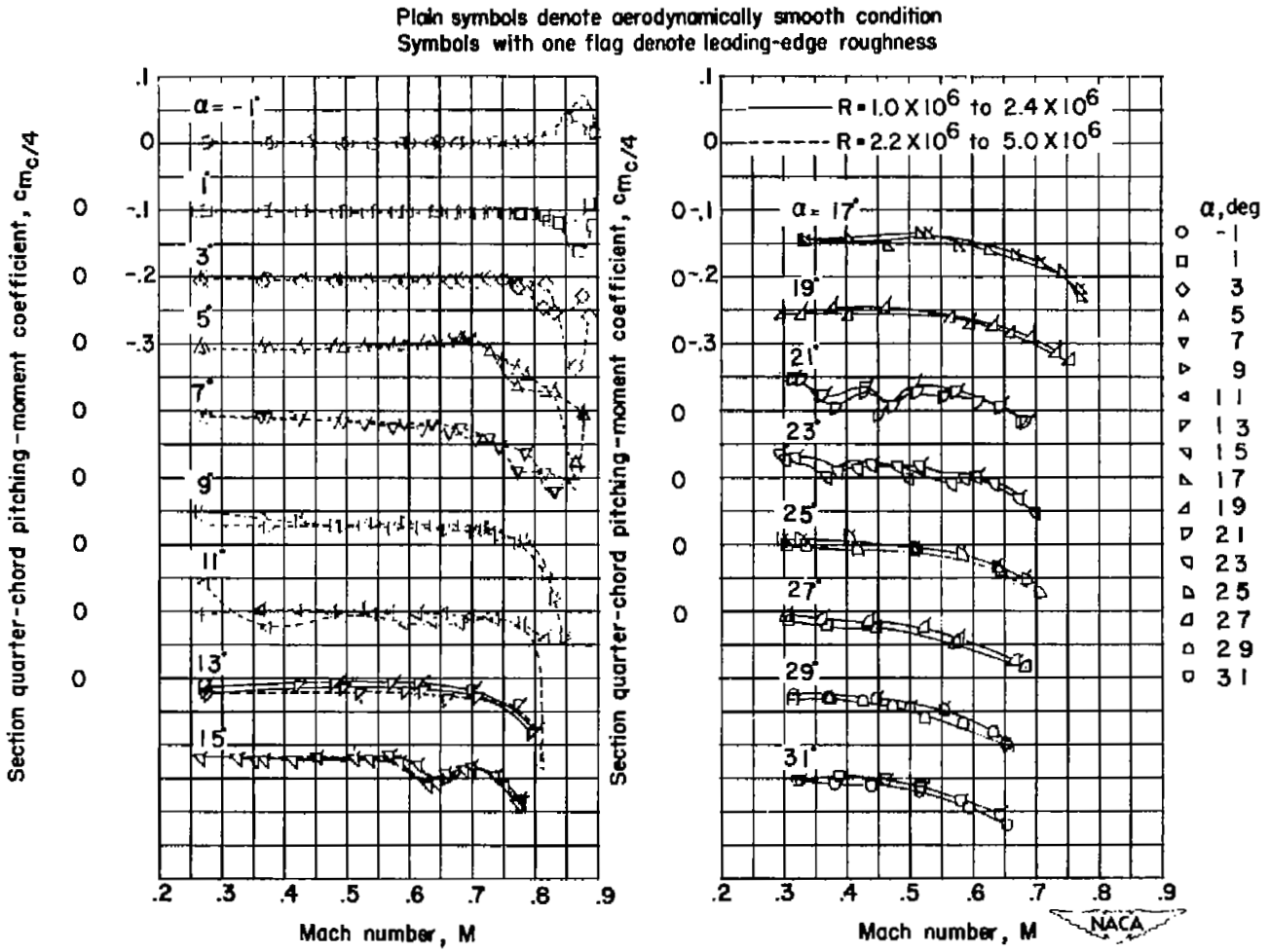

(c) Variation of section quarter-chord pitching-moment coefficient with free-stream Mach number.

Figure 6.- Concluded.

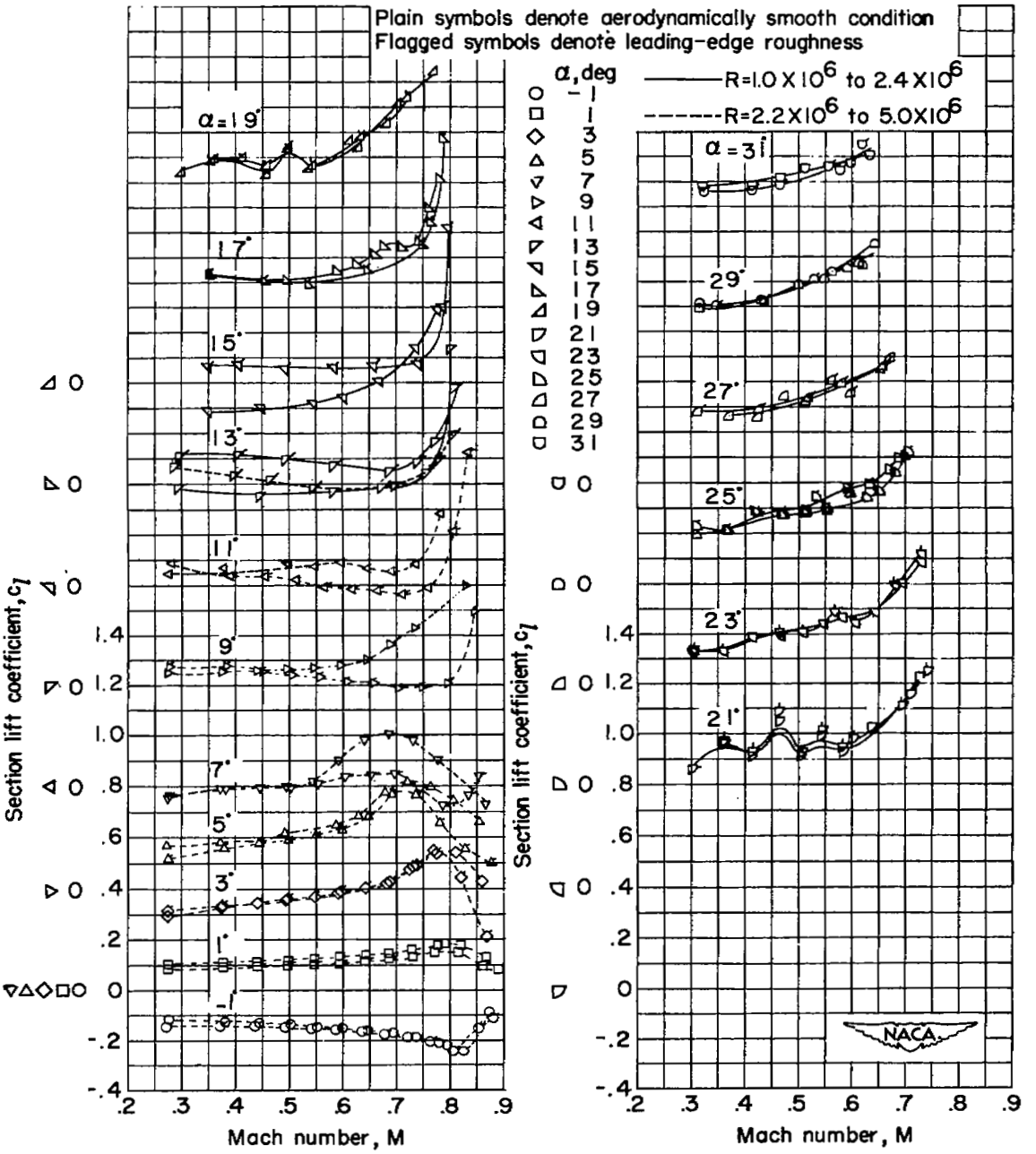

(a) Variation of section lift coefficient with free-stream Mach number.

Figure 7.- Effect of leading-edge roughness upon the high-speed aerodynamic characteristics of the NACA 64-010 airfoil section at various angles of attack.

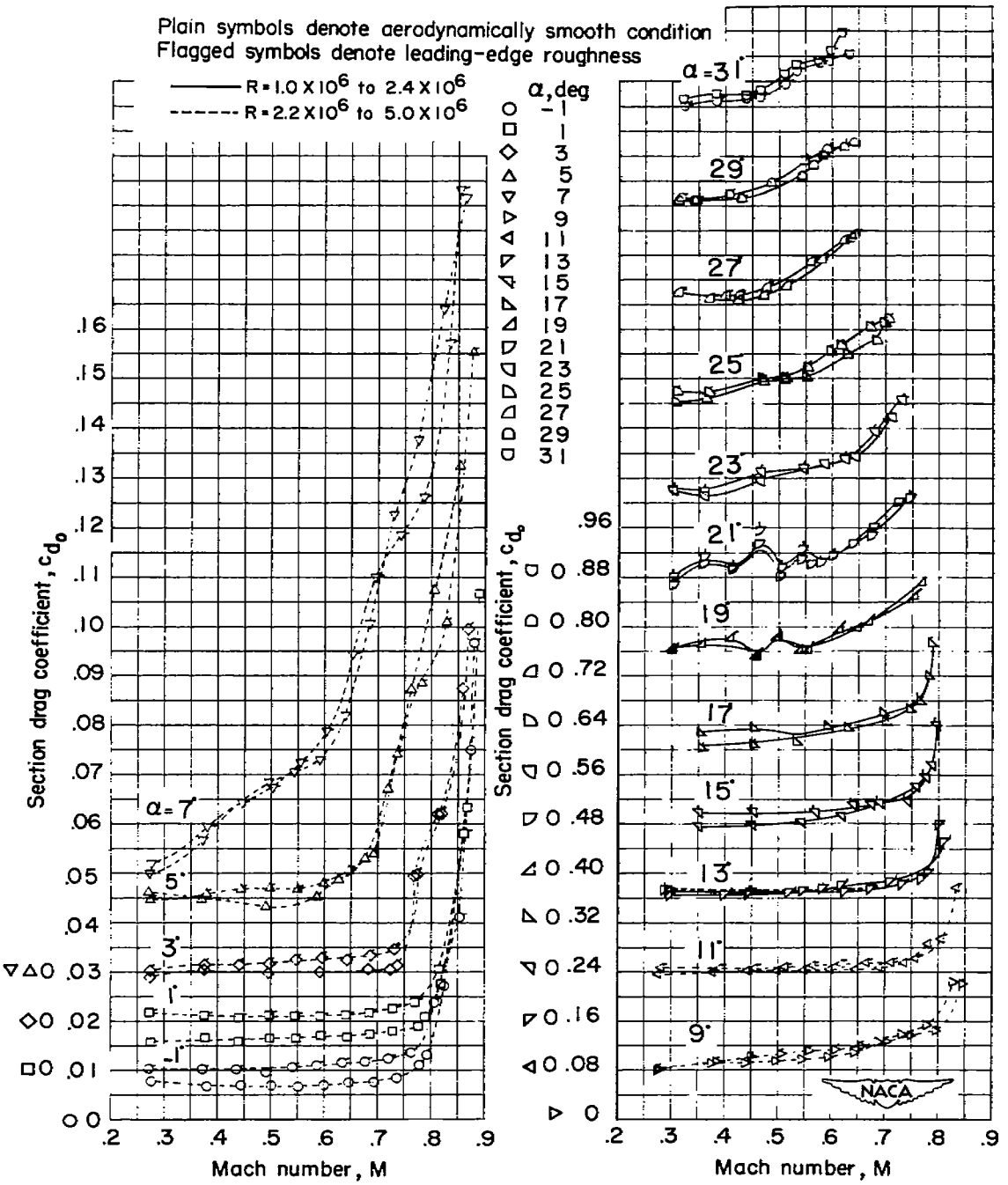

(b) Variation of section drag coefficient with free-stream Mach number.

Figure 7.- Continued.

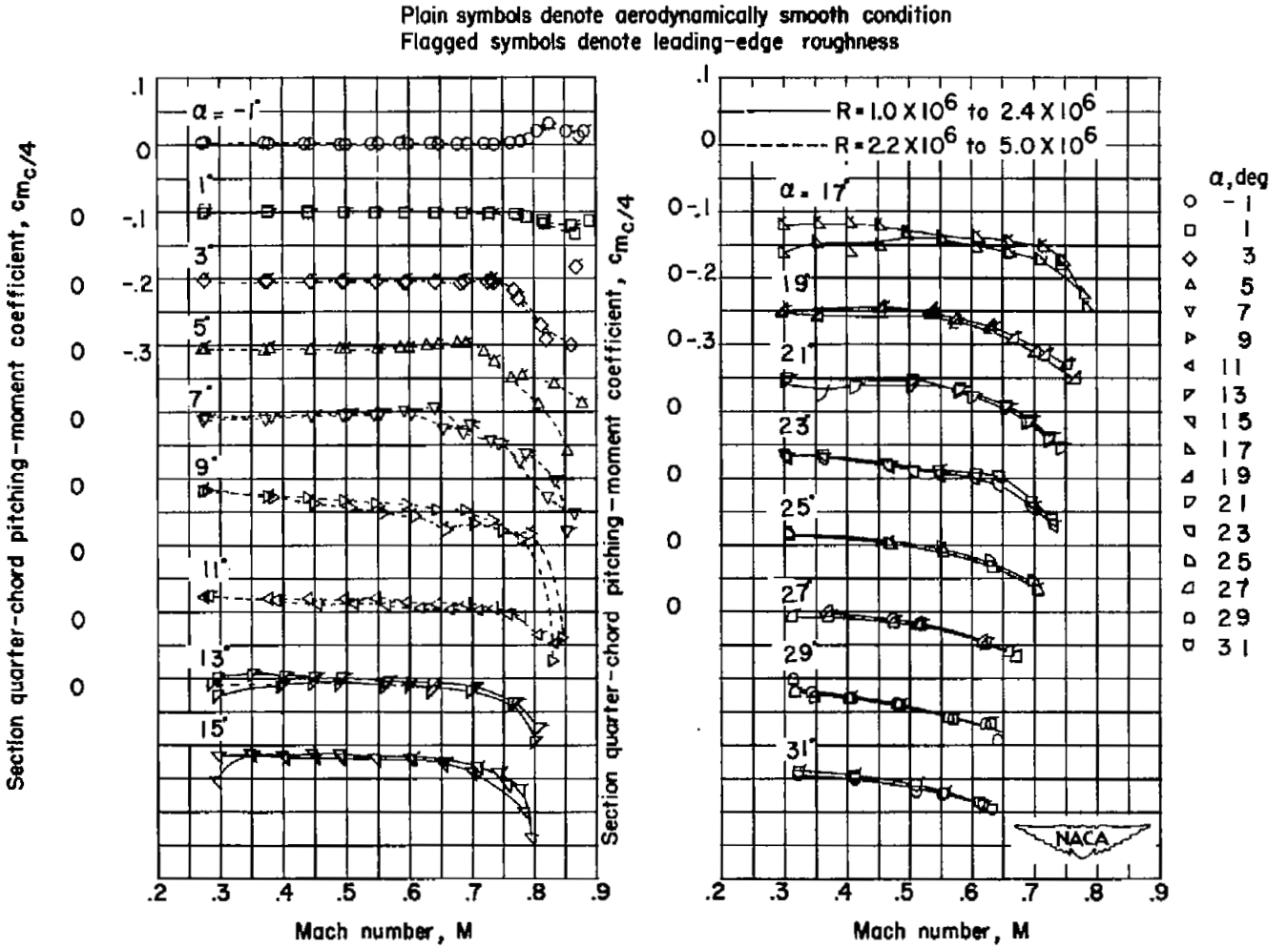

(c) Variation of section quarter-chord pitching-moment coefficient with free-stream Mach number.

Figure 7.- Concluded.

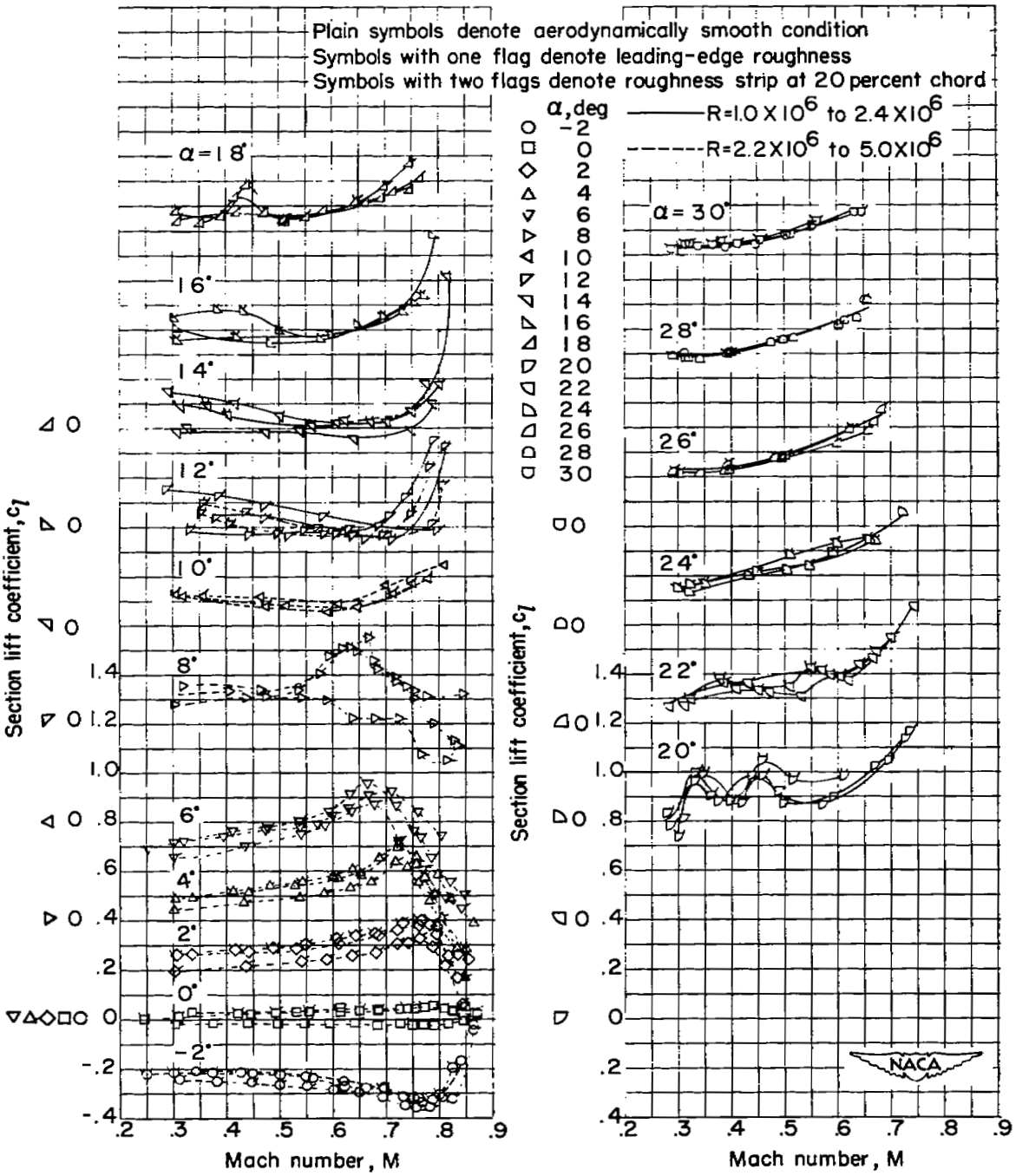

(a) Variation of section lift coefficient with free-stream Mach number.

Figure 8.- Effect of roughness upon the high-speed aerodynamic characteristics of the NACA 64_1-012 airfoil section at various angles of attack.

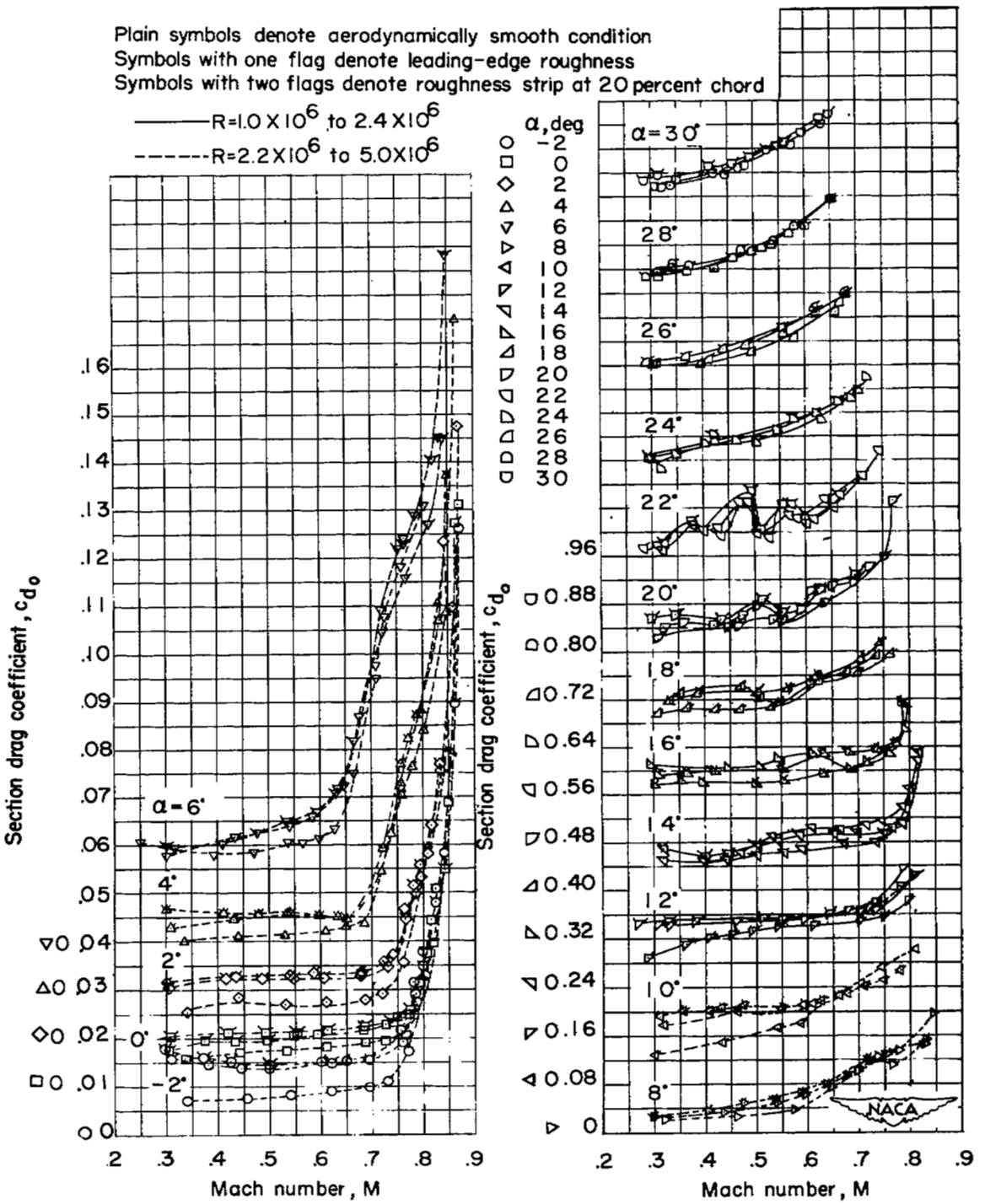

(b) Variation of section drag coefficient with free-stream Mach number.

Figure 8.- Continued.

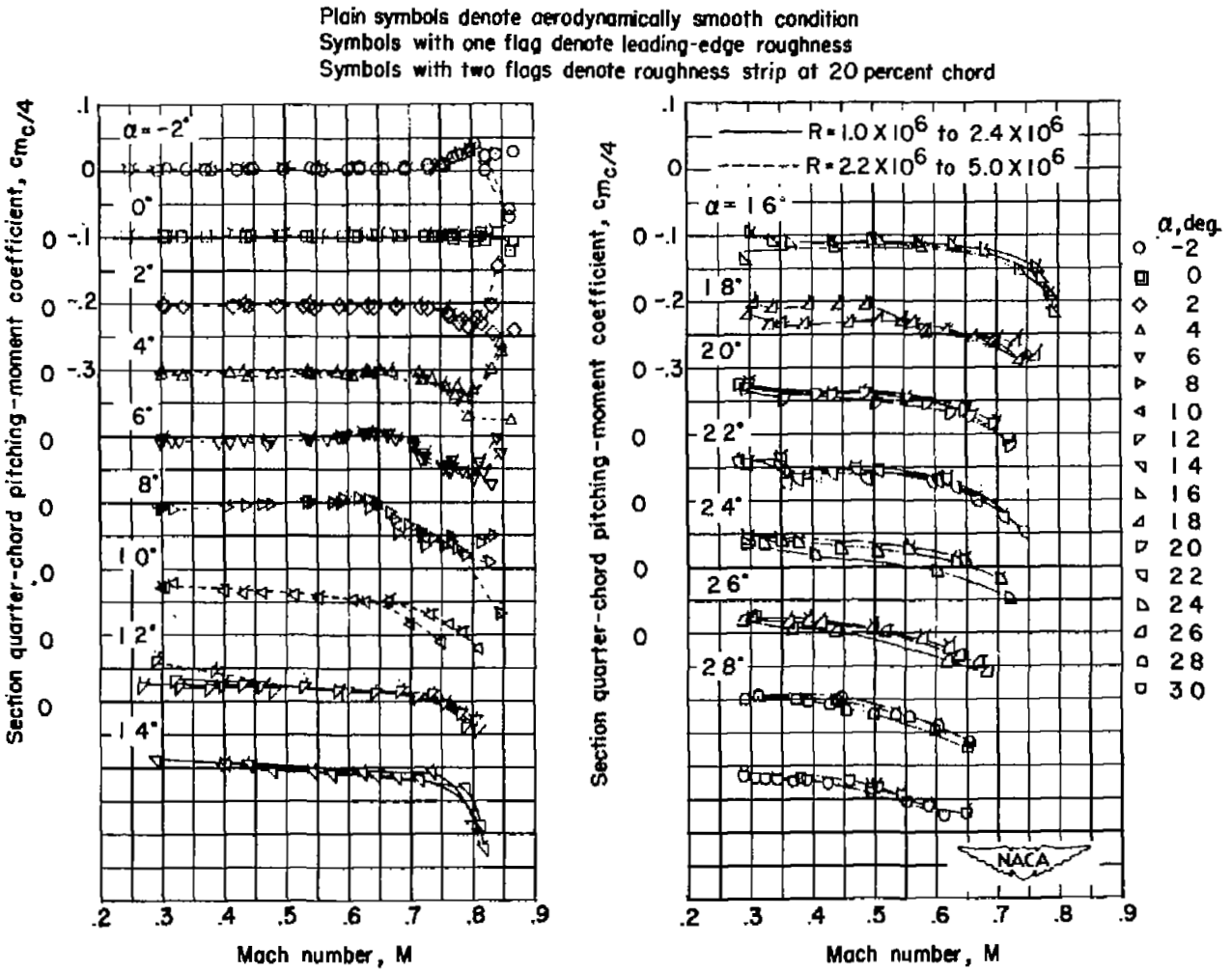

(c) Variation of section quarter-chord pitching-moment coefficient with free-stream Mach number.

Figure 8.- Concluded.

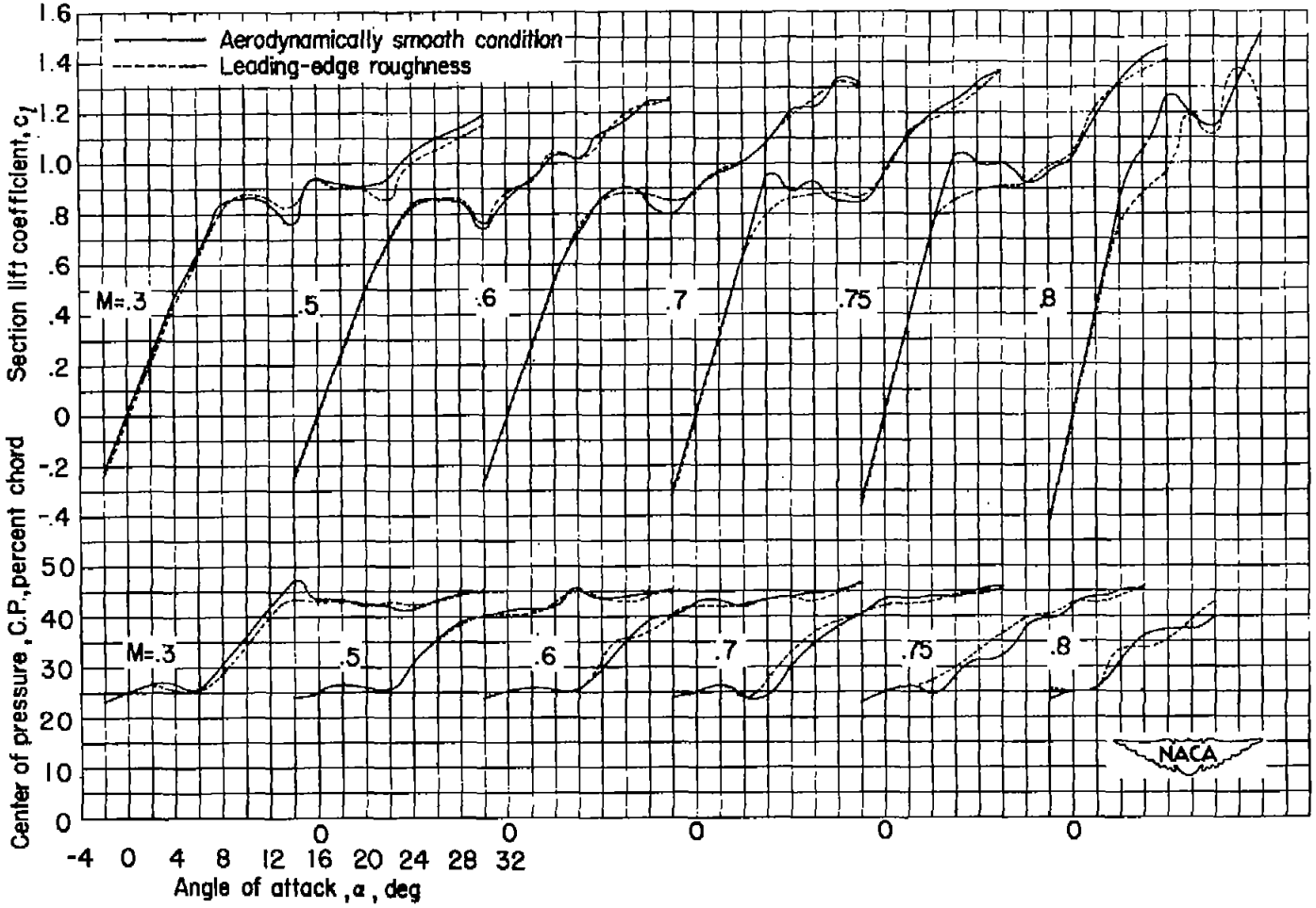

(a) NACA 64-006 airfoil section.

Figure 9.- Section lift coefficient and center of pressure as a function of section angle of attack for four airfoil sections at various free-stream Mach numbers.

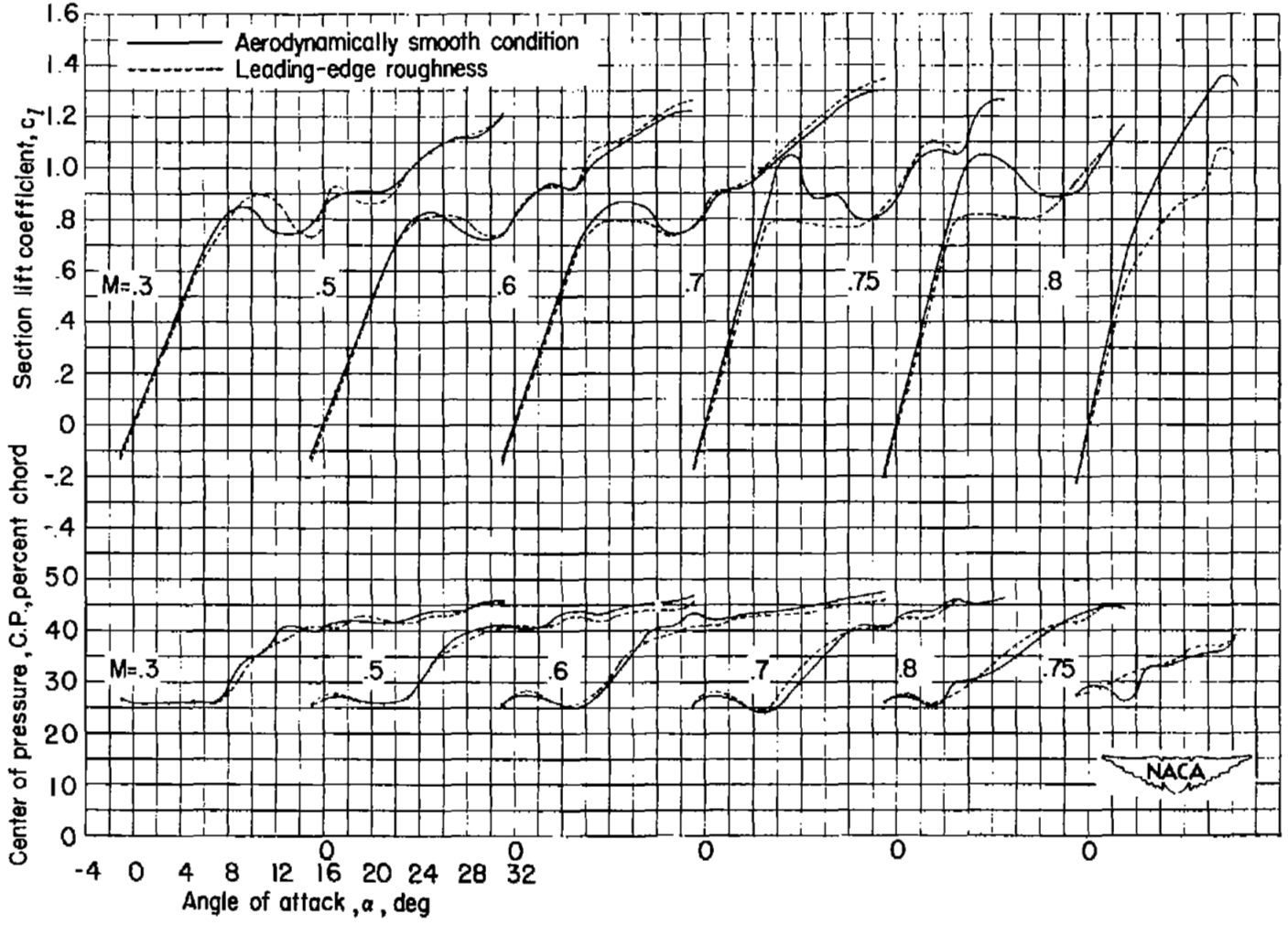

(b) NACA 64-008 airfoil section.

Figure 9.- Continued.

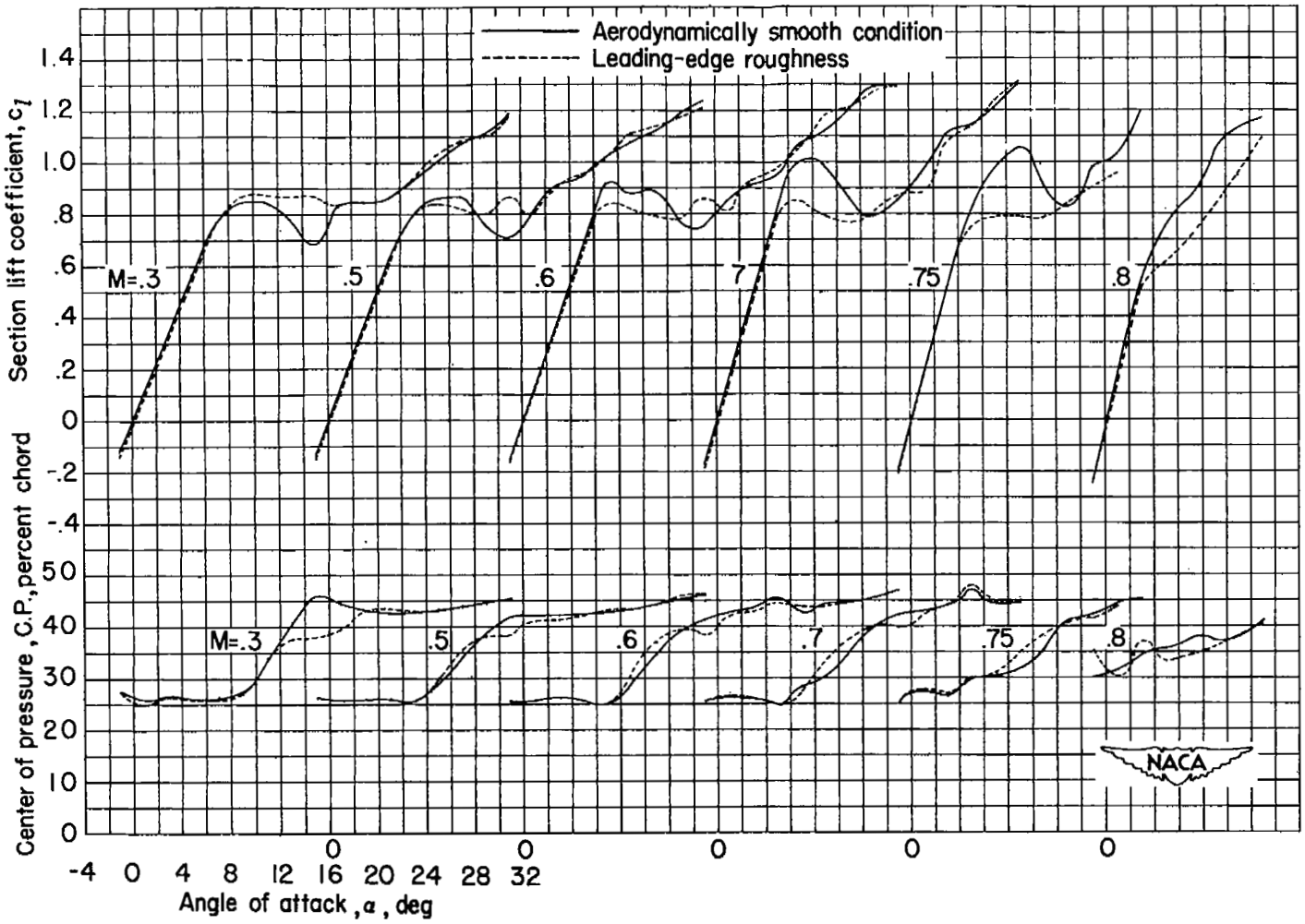

(c) NACA 64-010 airfoil section.

Figure 9.- Continued.

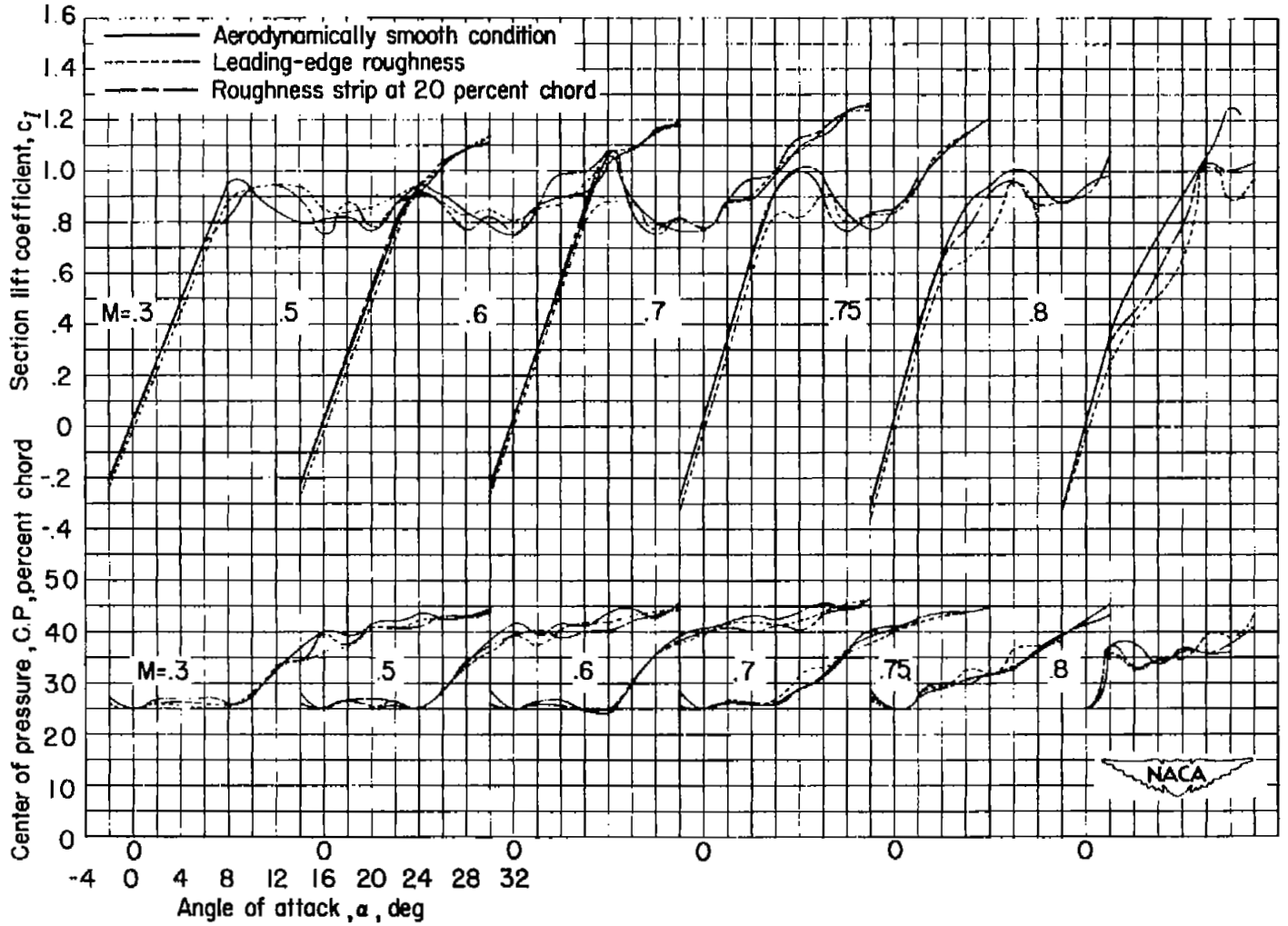

(d) NACA 64_1-012 airfoil section.

Figure 9.- Concluded.

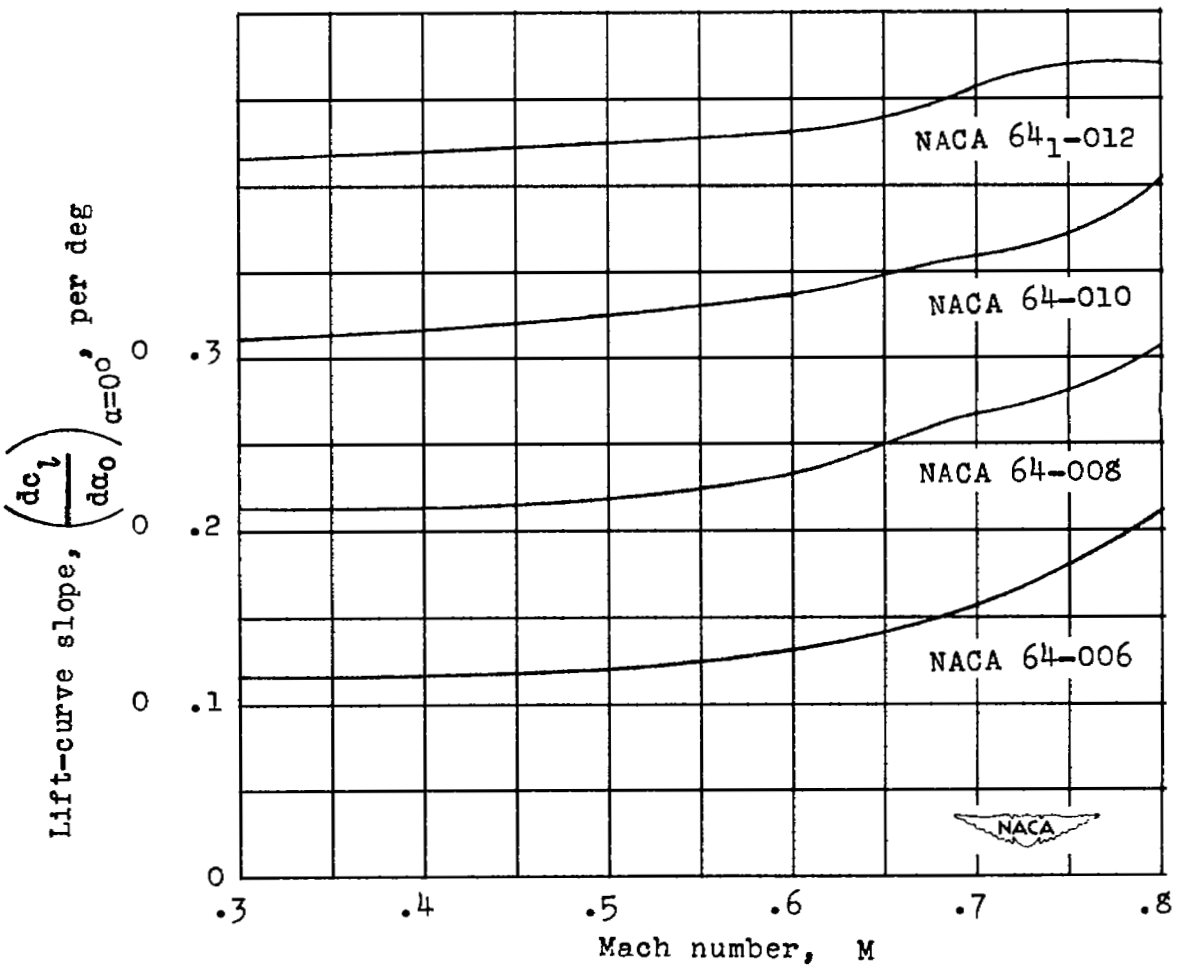

Figure 10.- Variation of the lift-curve slope with Mach number for the NACA 64-006, 64-008, 64-010, and 64_1-012 airfoil sections in the smooth condition.

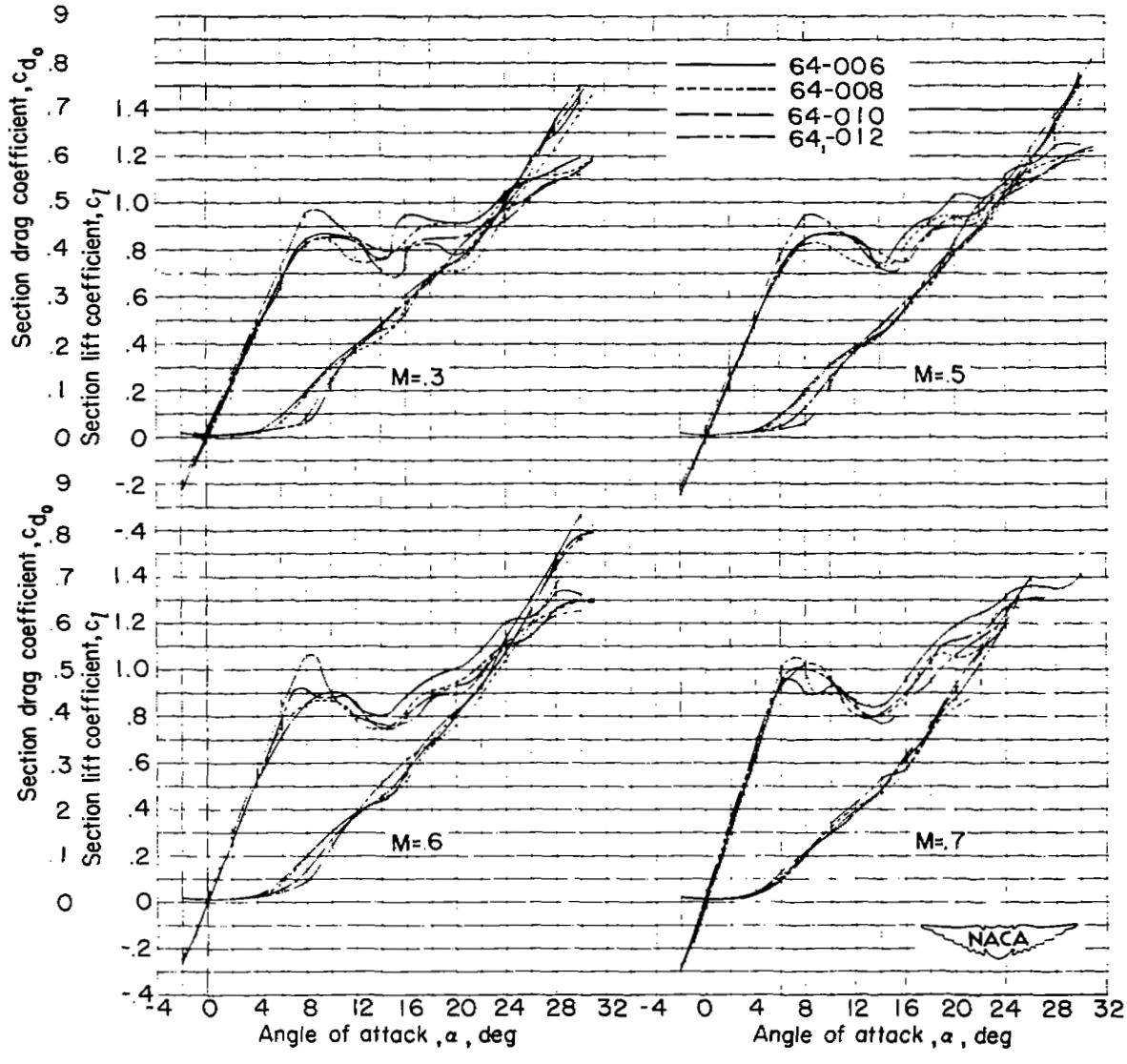

Figure 11.- Comparison of section lift and drag characteristics of the NACA 64-006, 64-008, 64-010, and 64_1-012 airfoil sections in the smooth condition for Reynolds numbers of 1.0×10^6 to 5.0×10^6 and various Mach numbers.

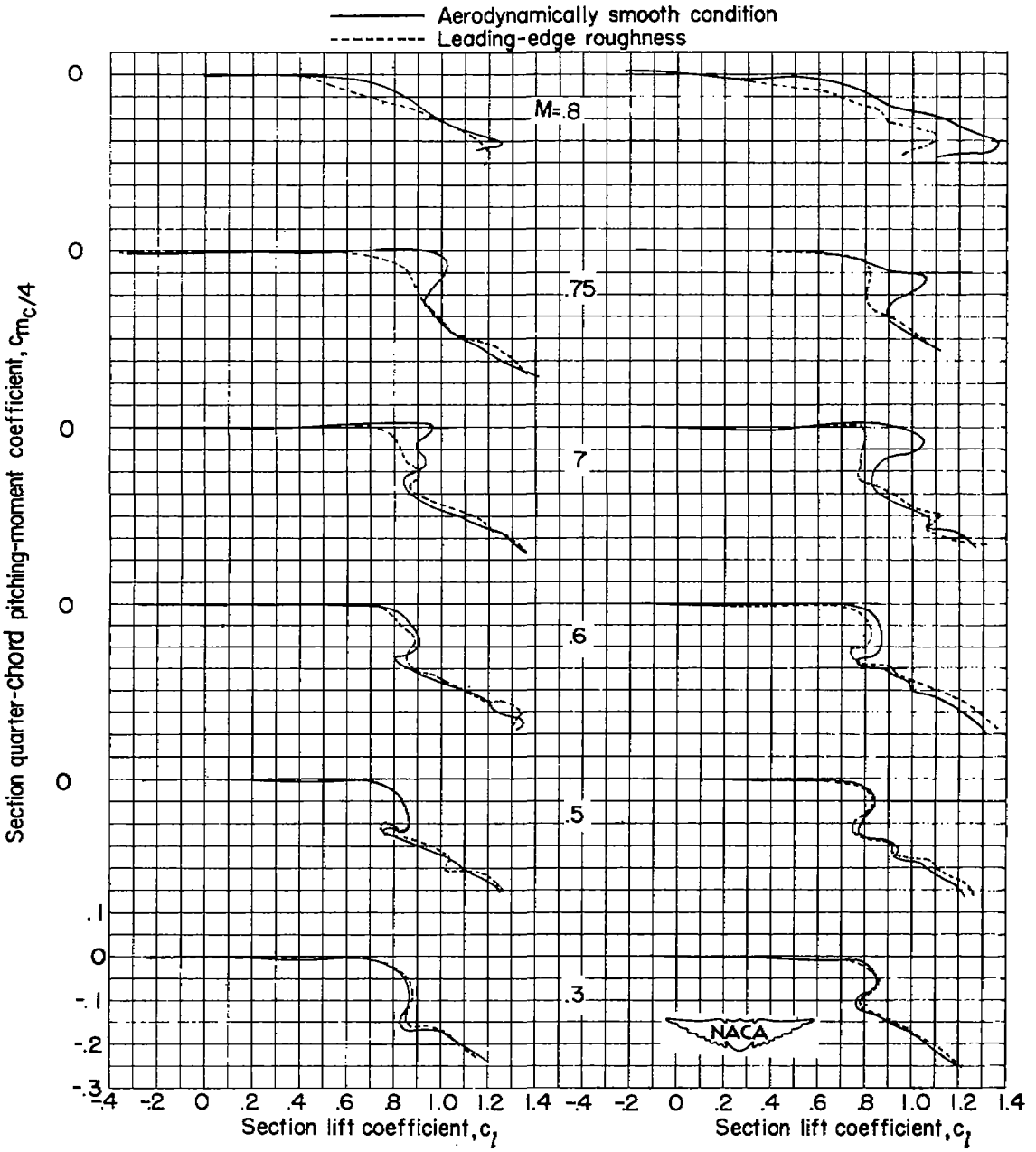

(a) NACA 64-006 section. (b) NACA 64-008 section.

Figure 12.- Section quarter-chord pitching-moment coefficient as a function of section lift coefficient for four airfoil sections at various free-stream Mach numbers.

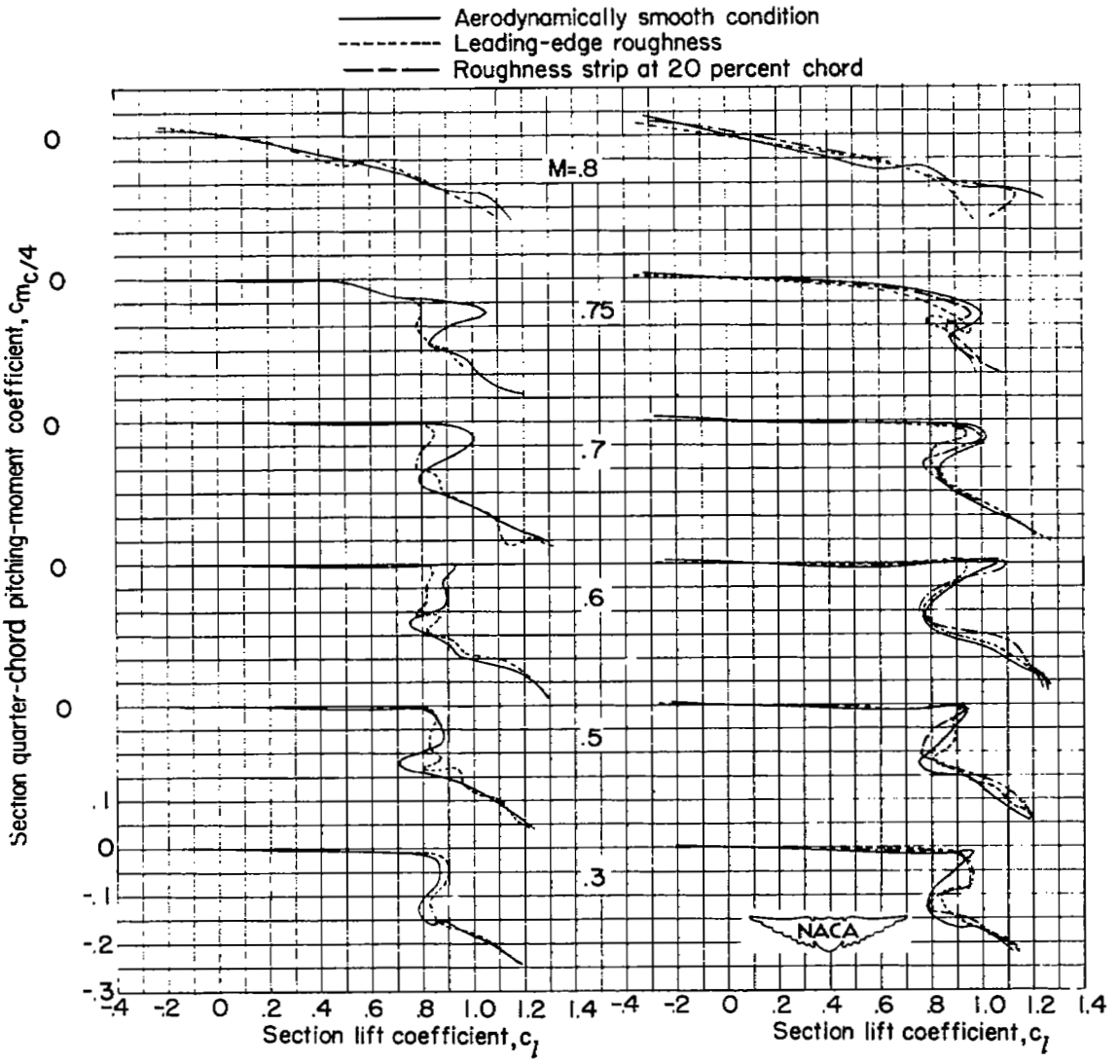

(c) NACA 64-010 section. (d) NACA 64_1-012 section.

Figure 12.- Concluded.

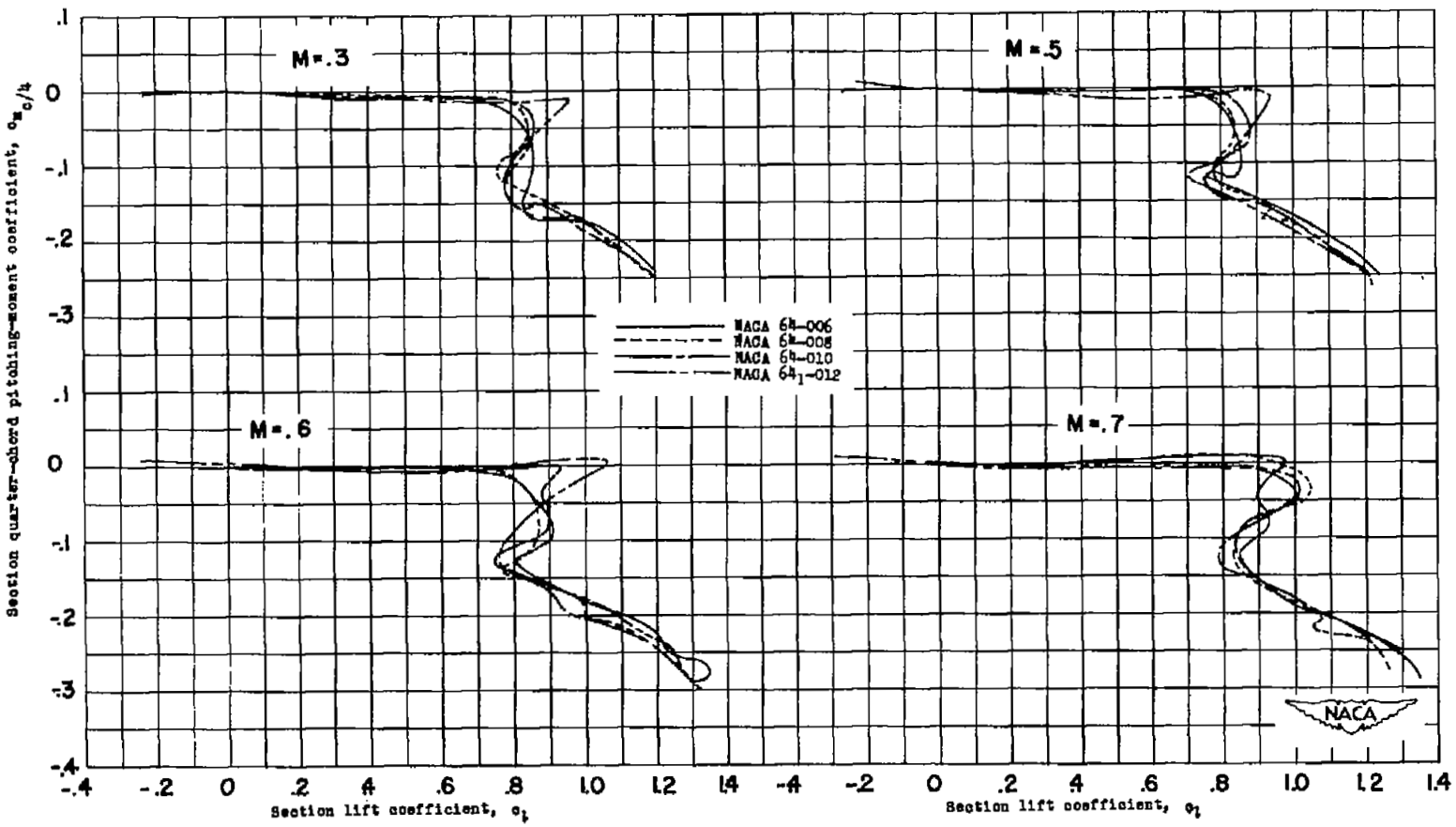

Figure 13.- Comparison of the section pitching-moment coefficient as a function of section lift coefficient for four NACA 6-series airfoil sections in the smooth condition at various free-stream Mach numbers and Reynolds numbers of 1.0×10^6 to 5.0×10^6.

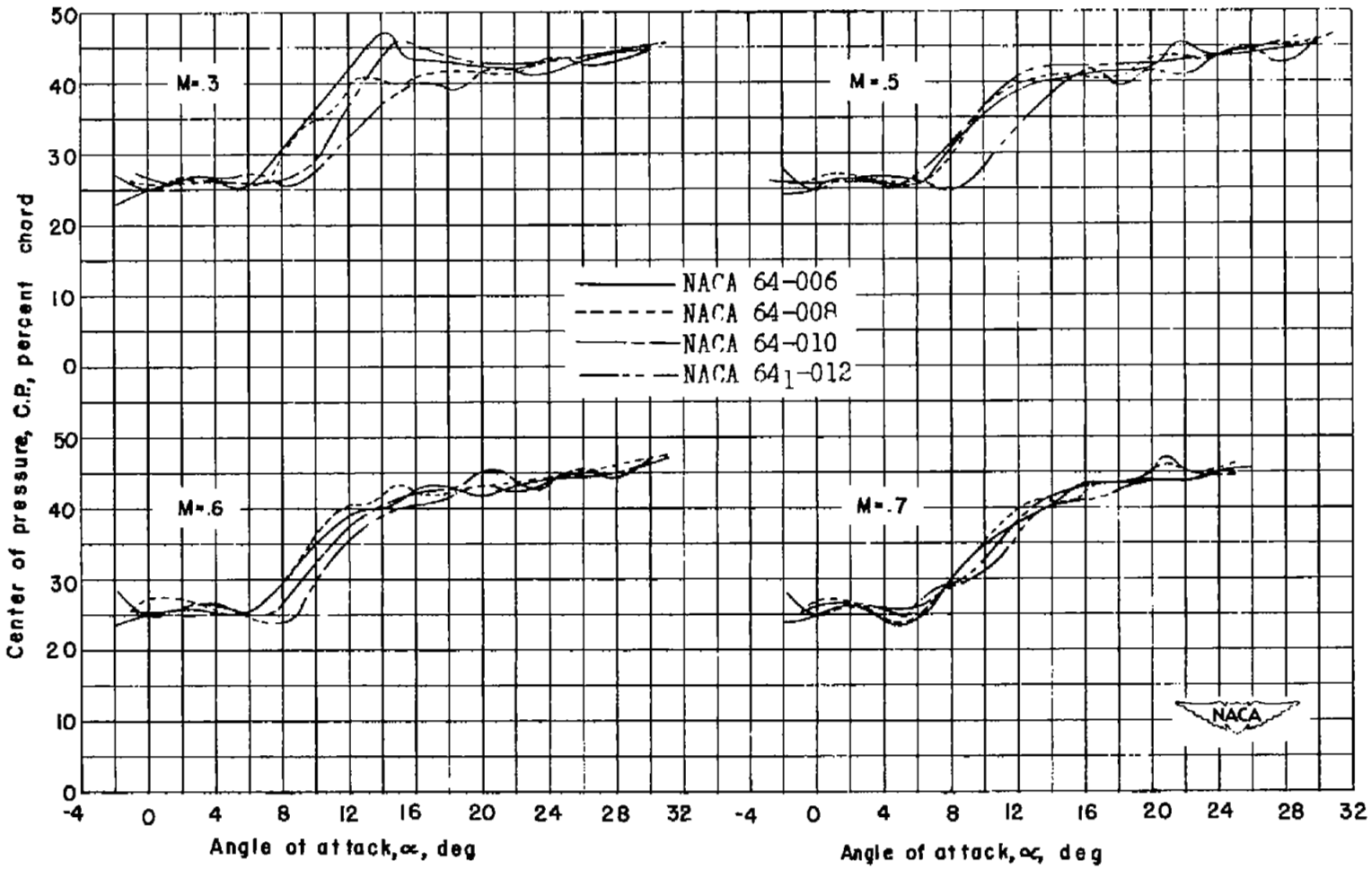

Figure 14.- Comparison of the section center-of-pressure characteristics for four NACA 6-series airfoil sections in the smooth condition at Reynolds numbers varying from 1.0×10^6 to 5.0×10^6 for several Mach numbers.

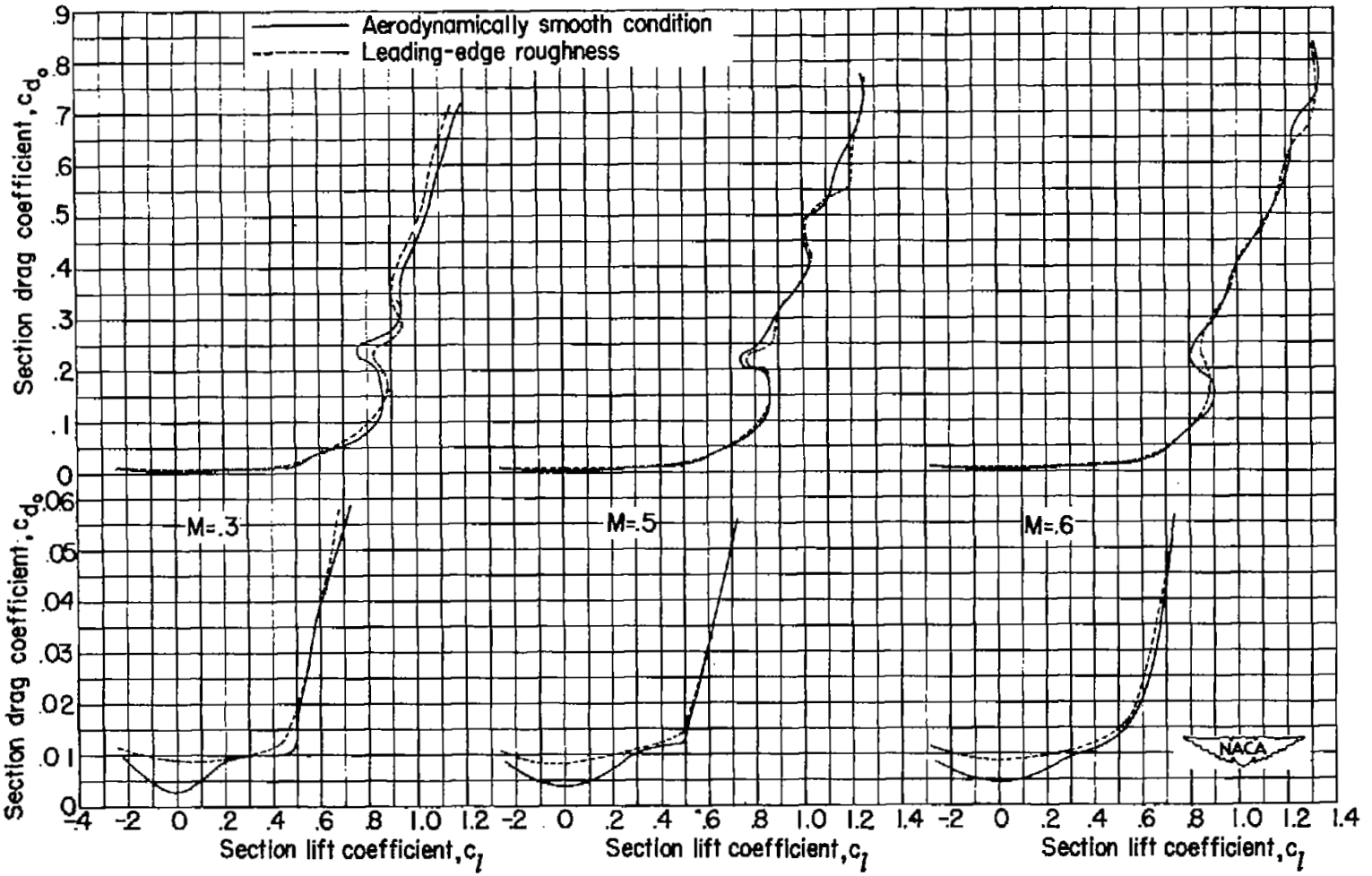

(a) NACA 64-006 airfoil section.

Figure 15.- Section drag coefficient as a function of section lift coefficient for four airfoil sections at various free-stream Mach numbers.

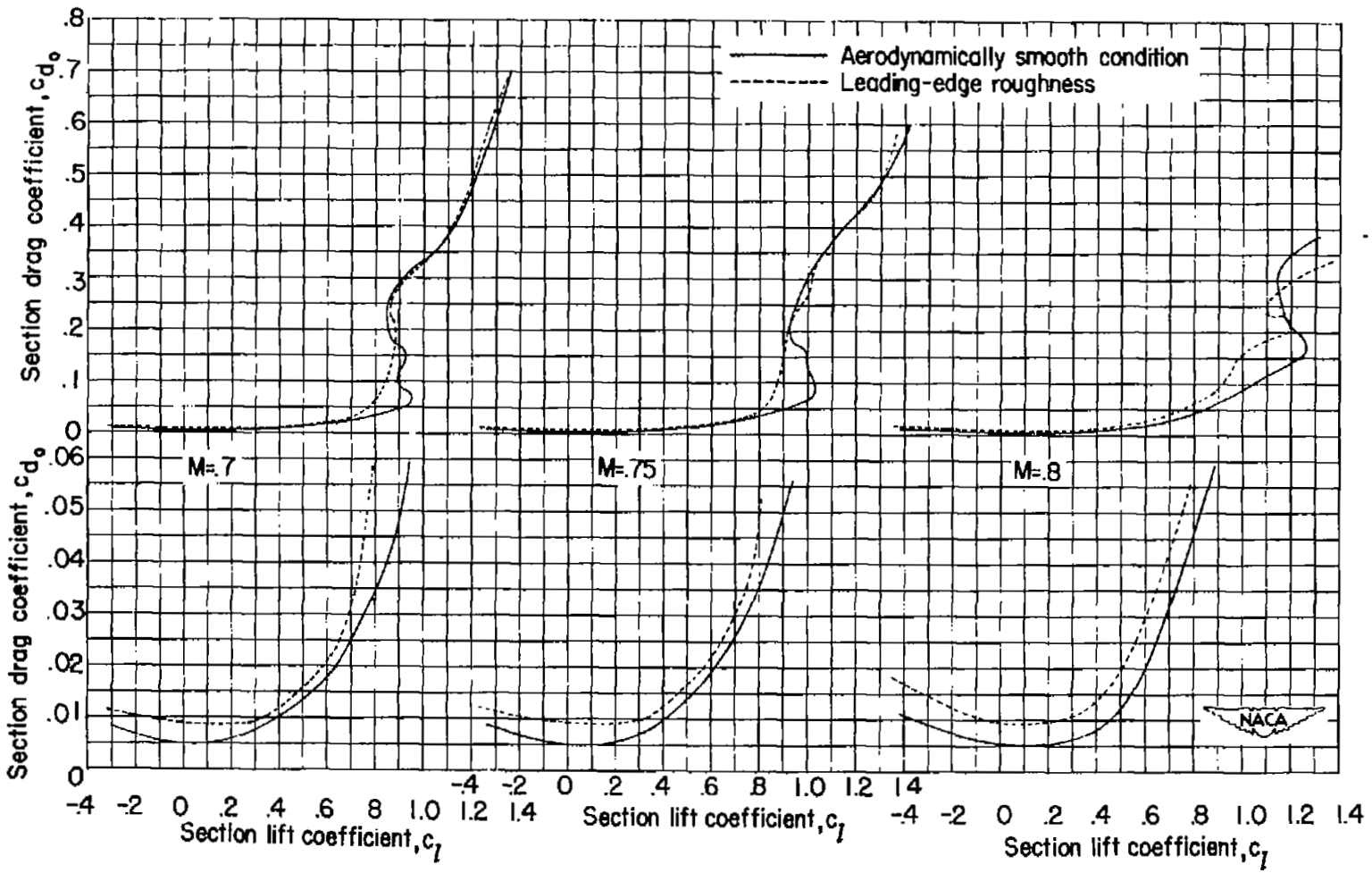

(a) NACA 64-006 airfoil section - Concluded.

Figure 15.- Continued.

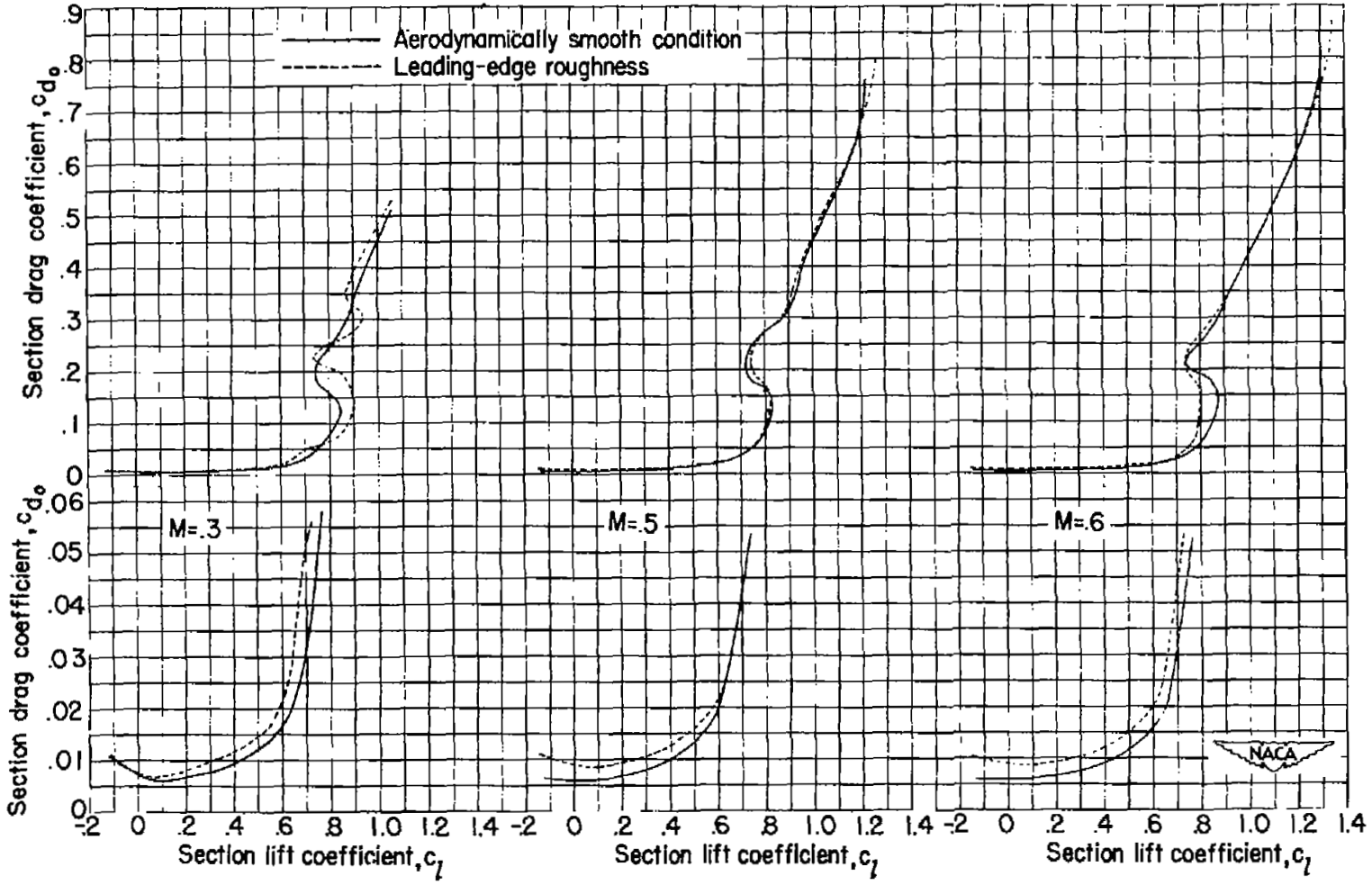

(b) NACA 64-008 airfoil section.

Figure 15.- Continued.

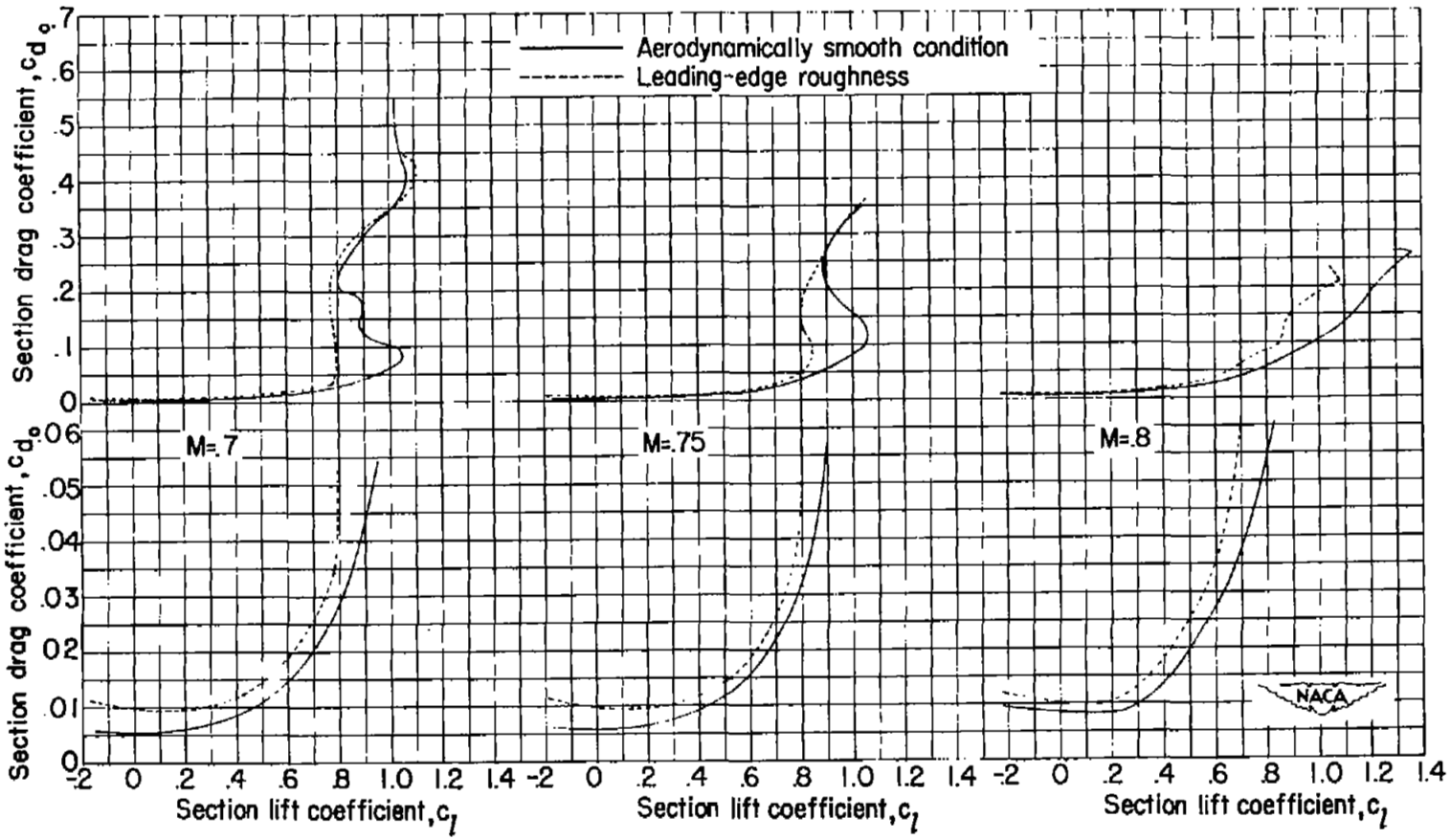

(b) NACA 64-008 airfoil section - Concluded.

Figure 15.- Continued.

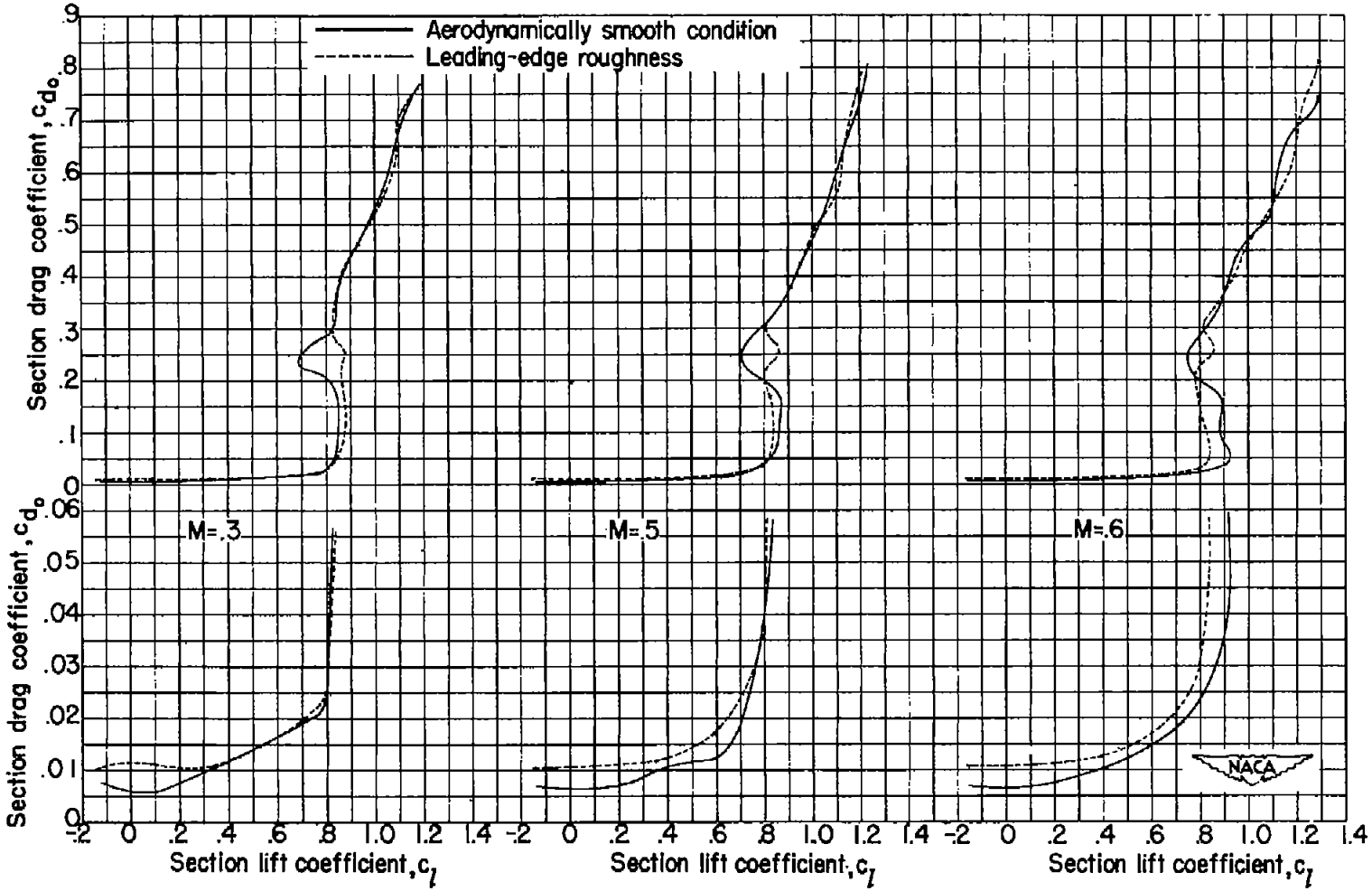

(c) NACA 64-010 airfoil section.

Figure 15.- Continued.

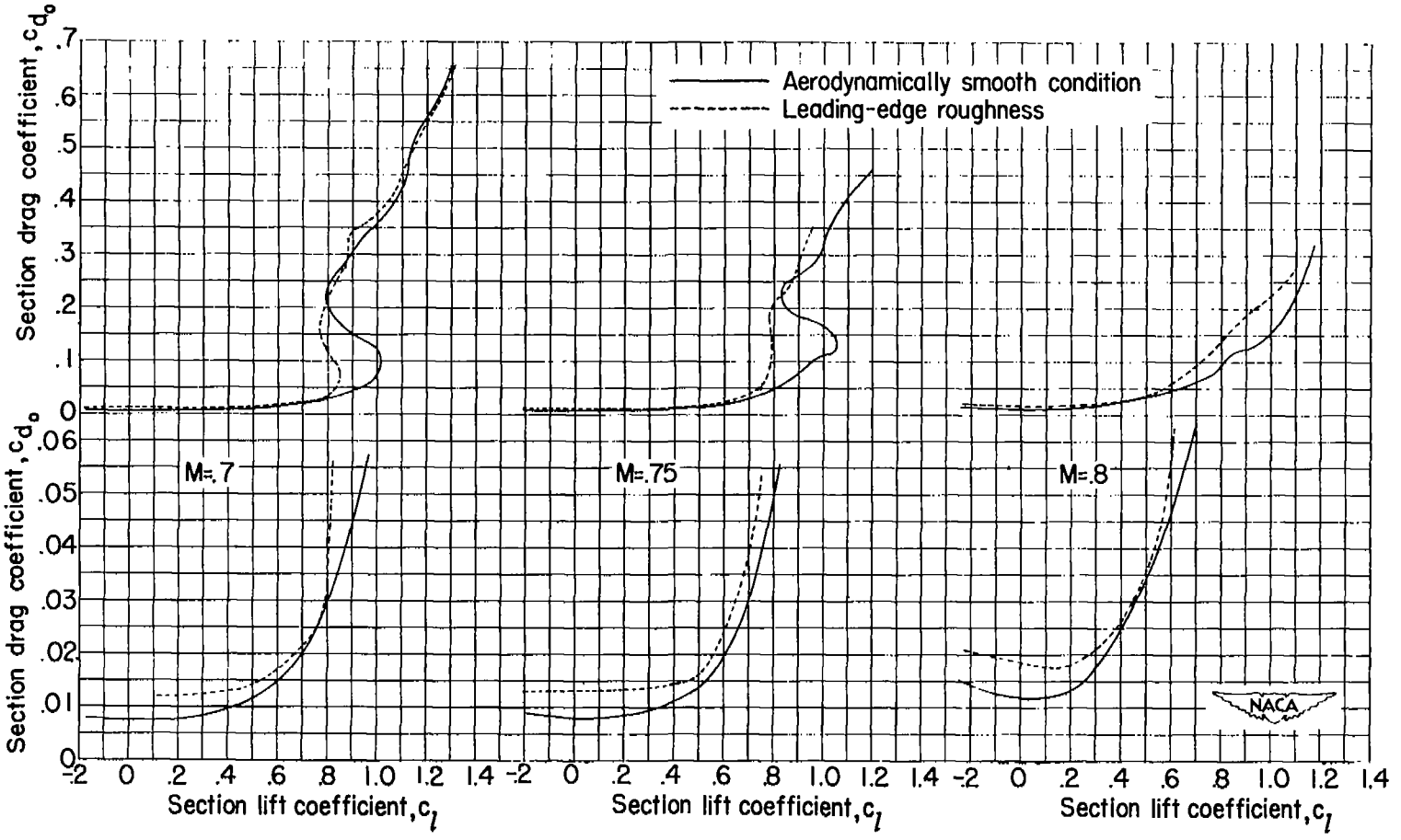

(c) NACA 64-010 airfoil section - Concluded.

Figure 15.- Continued.

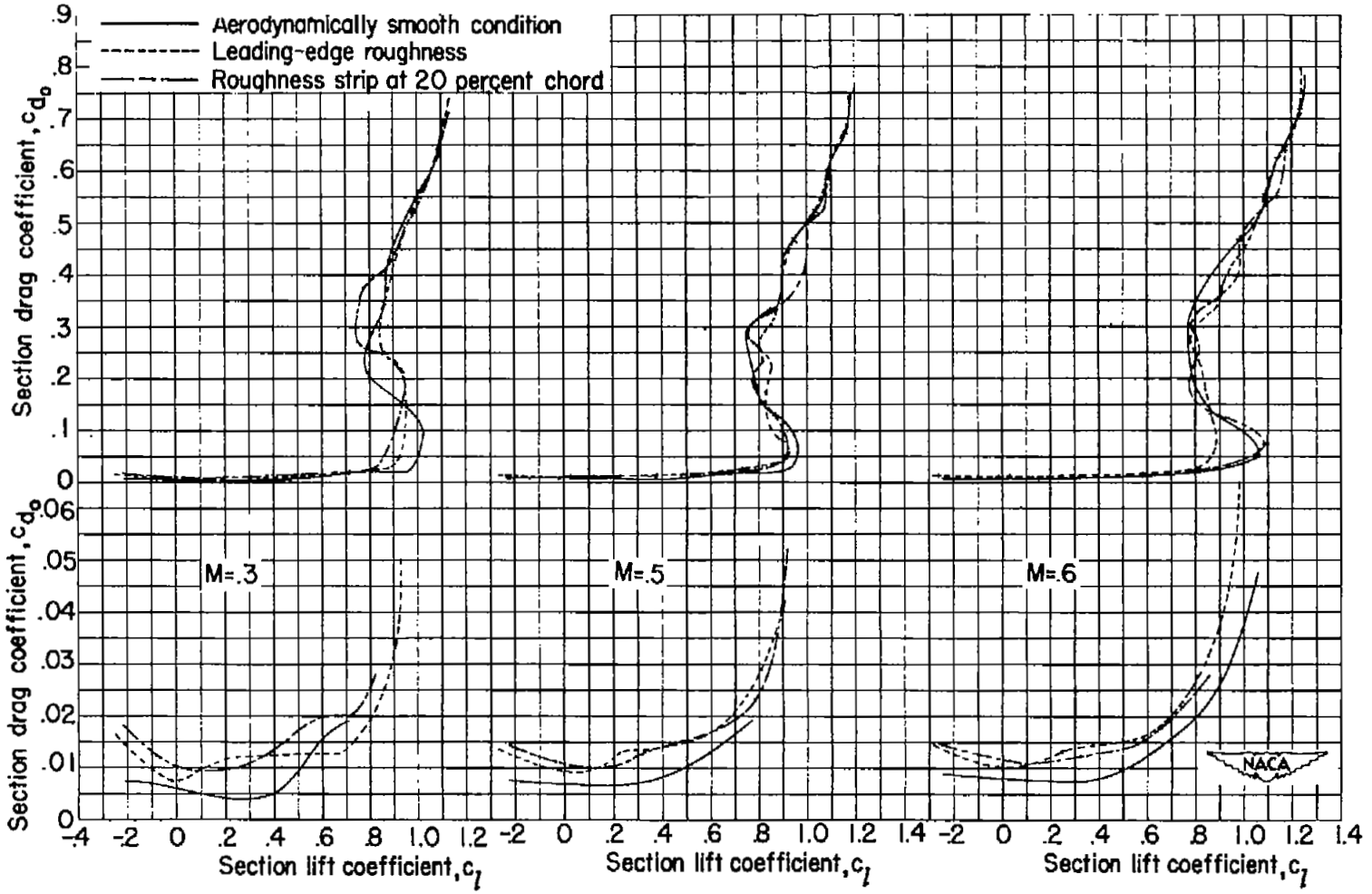

(d) NACA 64_1-012 airfoil section.

Figure 15.- Continued.

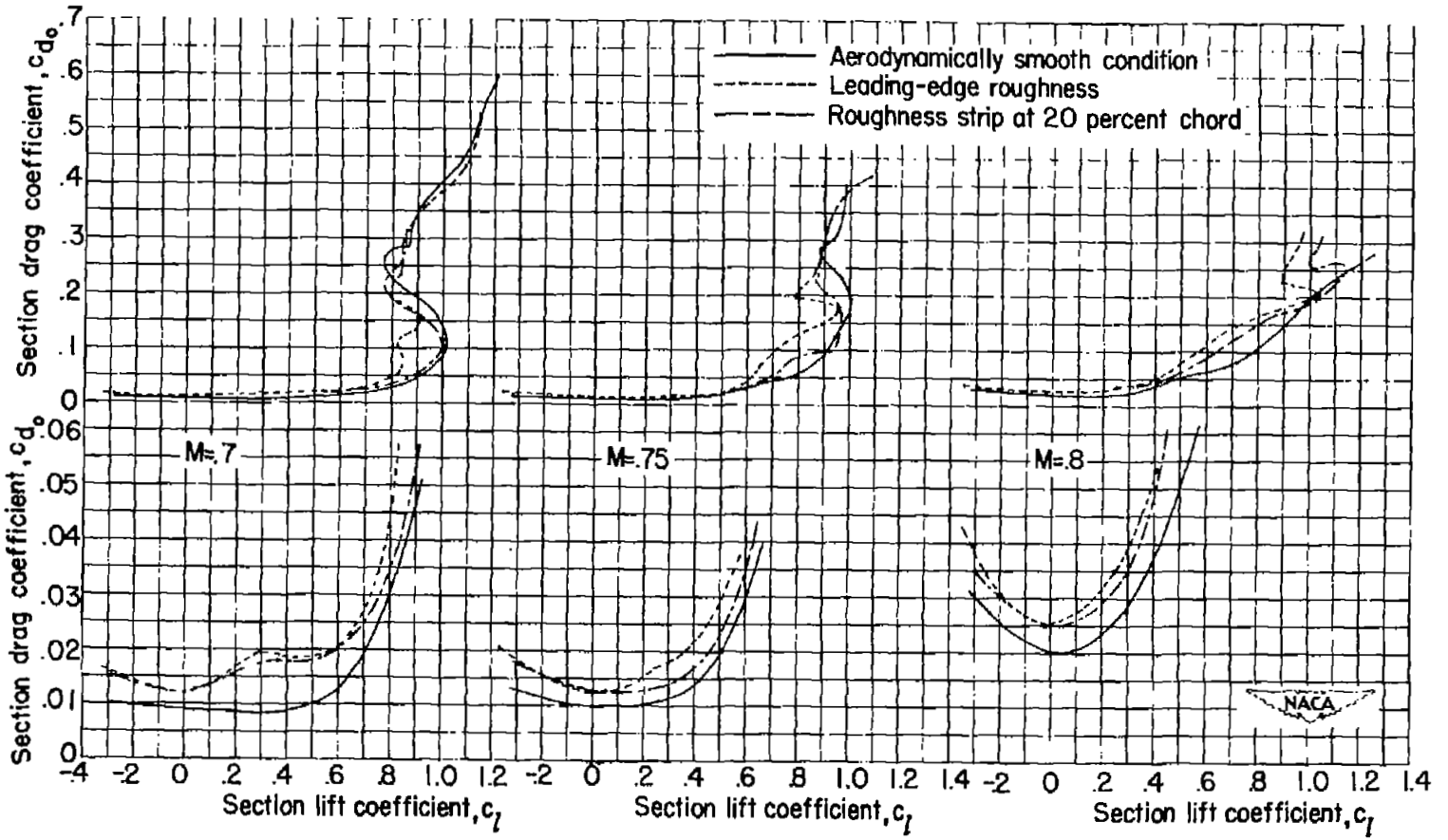

(d) NACA 64_1-012 airfoil section - Concluded.

Figure 15.- Concluded.

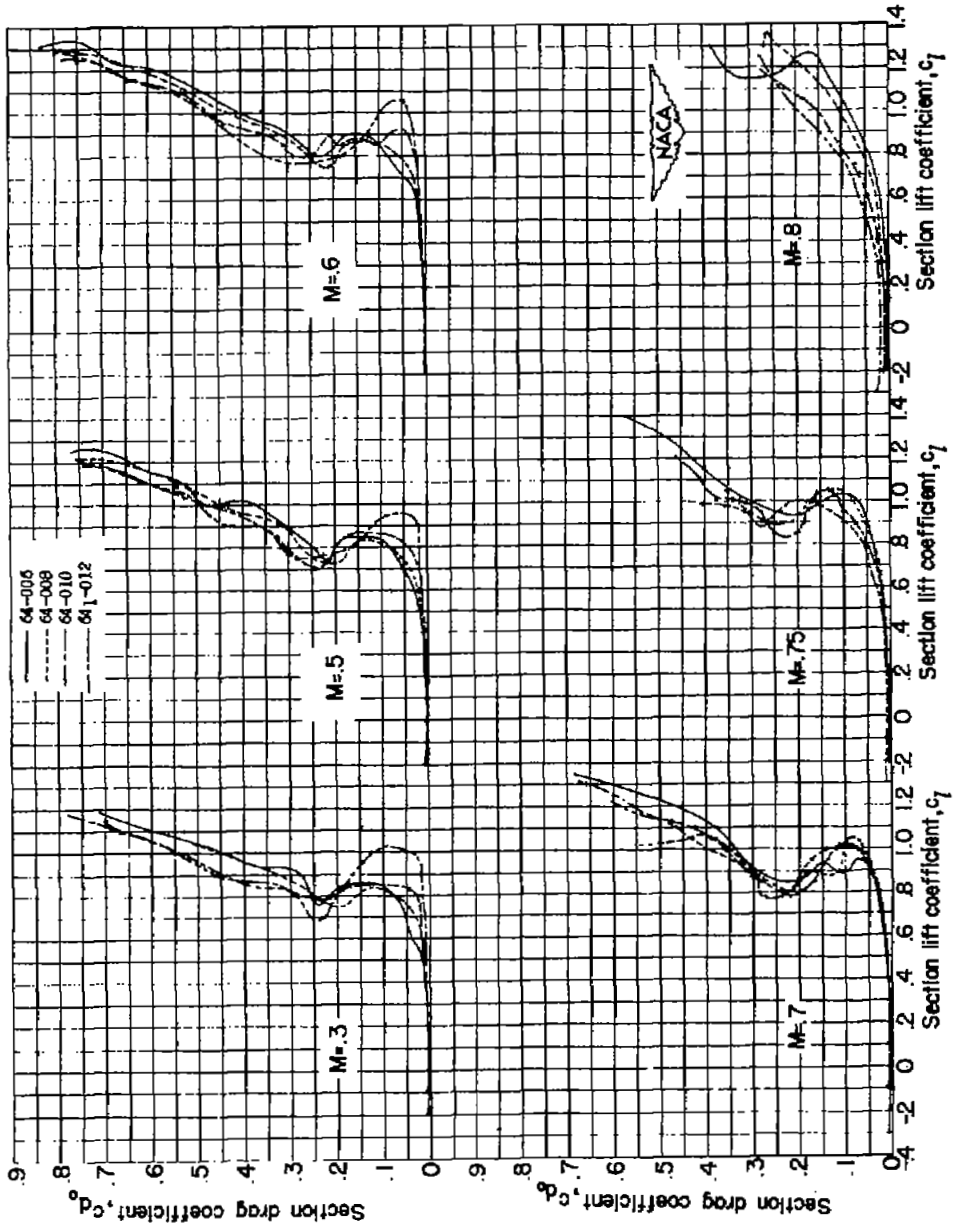

Figure 16.- Comparison of the section drag coefficient as a function of section lift coefficient for four NACA 6-series airfoil sections in the smooth condition at various free-stream Mach numbers and Reynolds numbers of 1.0×10^6 to 5.0×10^6.

NACA-Langley - 6-8-53 - 335